SUBIMAGE REGISTRATION BASED ON CANDIDATE SELECTION AND MULTIPLE CORRESPONDENCES

MASTER DEGREE FINAL PROJECT

Victoria Amado Cepeda

Directed by Dr.Francesc Serratosa
Co-Directed by Carlos Francisco Moreno García

Master Program
Computer Engineering: Computer Security and Intelligent Systems

UNIVERSITAT ROVIRA I VIRGILI

Tarragona
2014

CONTENTS

LIST OF FIGURES

LIST OF TABLES

CHAPTER I

1. INTRODUCTION

During the last decades, image analysis has presented great advances, such as imaging devices and sophisticated algorithms for image analysis, applied in different areas such as computer vision, medicine, cartography, forence and etc. [1][2]. One step of great importance in this analysis is image registration, the process by which point-by-point correspondence of two images is determined verifying which parts of a reference image correspond to which parts of the sensed image. This helps solving problems of different processes in computer vision, such as scene reconstruction, object recognition and tracking and retrieval of images.

There are two steps involved in the solution of the image registration problem are the following [3]. First, some salient points are selected from both images[4] and a set of tentative matches between these sets of points is computed [5][6]. Tentative correspondences may be computed either on the basis of correlations measures or feature-descriptor distance. Second, these tentative matches can be further refined by a process of outlier rejection that eliminates the spurious correspondences or alternatively [7], uses them as starting point of some optimization scheme to find a different and more consistent set [8].

However, in some areas of implementation, image-registration (forensic palmprint recognition, satellite images.) is more usual to detect a partial or small picture that a complete picture of the scene. In these cases, the returned correlation in the first step of the processes fails due to the large amount of outliers generated by comparing the small picture (reference image) with the full image (sensed image) outliers. Therefore, the second step depends greatly on the previous step. If it is unable to recover the transformation matrix of the small image into the large image, then there is no guarantee of success.

For this reason, we need to implement an image registration algorithm. This method be applied mainly on forensic palmprint recognition, because in this field it is more usual to find a poor quality images and small parts of a whole picture. Not within the implementation would deepen the extraction of the points of the respective images, as this process has made great progress and developments. The method is based on the use of minutiae, since it is more likely to get a more real correspondence using these features.

This thesis is organized as follows: Chapter 2 introduces a state of the art of different topics of biometrics palmprint in forensic analysis. Chapter 3 presents our proposal and describes the algorithm implemented for partial to full image registration based on candidate positions and multiple correspondences. Chapter 4 describes our practical evaluation of method. Finally, the Chapter 5 presents the reports some conclusions and remarks on this proposal.

CHAPTER II

2. STATE OF THE ART

2.1. Biometric system

Biometrics refers to recognize or identify an individual based in different characteristics, such as physical, chemical or behavioral (e.g., face, fingerprint, hand geometry, palmprint, iris, keystroke, signature, voice and gait) [9]. In the modern society biometrics techniques have been relevant because of the need different identity management systems, whose functionality relies on the accurate determination of an individual's identity in the context of several different applications. Examples of these applications include forensic analysis (as authenticate a person or identify people who left trails in a crime scene), sharing networked computer resource, grating access of different entities, amongst others.

Every image registration process is formed by architecture, and biometrics systems are no exception. Figure 1 shows the typical architecture are formed by following stages: 1) *Data acquisition* (Obtained from an input device), 2) *Image preprocessing* (Is performed in this stage, including segmentation, noise reduction, and rotation and translation normalization), 3) *Feature Extraction* (Posses the stable and unique properties of low intra-class difference and high inter-class difference, 4) *Feature matching* (Is a matching score obtained by matching the identification template against the master templates. If the score is less than a given threshold, the user is authenticated).

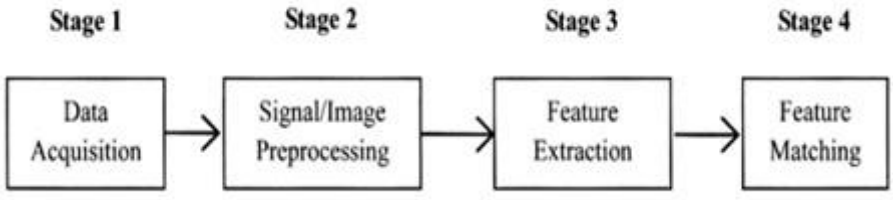

Figure 1 Architecture biometrics systems

Depending the application context, the biometric systems usually operate in three modes: enrollment, identification, and verification (some systems, however, only have either identification or verification[9]). The stages in everyone mode, as show of Figure 2, are Enrollment Process, Verification Process, and finally, Identification Process [10].

- **Enrollment:** This process implemented is before an individual can be verified or identified by the system. The user's biometric data is captured, preprocessed and feature- extracted. The user's template is then stored in a database or file system.
- **Identification:** This refers to making recognition of an individual by searching the entire template database for a match (one to many).
- **Verification:** This refers to the recognition of person's identity by comparing the captured biometric characteristics with his or her own biometric template pre-stored in the system (one to one).

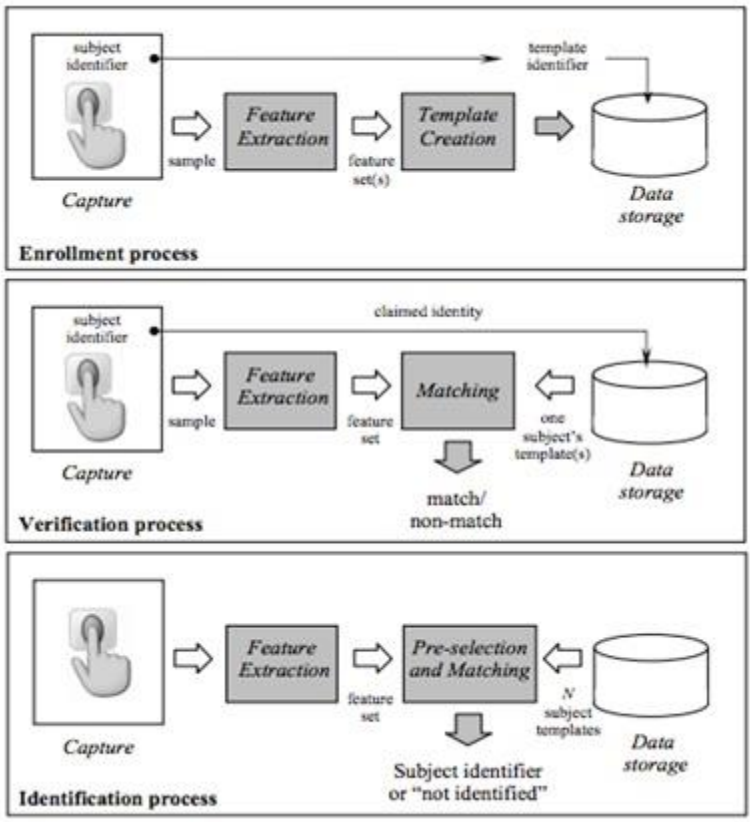

Figure 2 Enrollment and recognition (verification and identification) stages of biometrics system

The use of biometric systems depends directly on the application for which it intends to be used. The selection of features and mode of operation are important steps in these applications. There are several fields, such as commercial use, governmental and forensics. For this work, we focus on the latter area.

Among all biometric identification systems, the most popular one is the fingerprint. However one problem is that fingerprints of a significant fraction of the population may be unsuitable for automatic identification, because of genetic factors, aging, environmental, or occupational reasons [10]. Palmprint based system are being now considered, as hand palms provide surface area than fingers, large amounts if identifying features could be extracted, such as ridges and valleys. In comparison to fingerprints, the palm of hand is the biometric characterization is more complete[9]. Also, the palms contain additional distinctive features such as principal lines, wrinkles, delta points, and datum points which can be captured even with a lower resolution scanner [11].

2.2. Palmprint Recognition

Recently, more and more systems include images of the hand because of the great advantages that these conveys, as hands are rich in different characteristics. Palmprint recognition is the process connected to the skin patterns of the palm, composed of lines, point, and texture. Palmprints may be found on the surface of an object, mainly due to perspiration. The study of palmprint can be divided into in forensic and non-forensic. The first, referred to a palmprint found on a crime scene and the second a study that may use imaging techniques to obtain observable features of a palm.

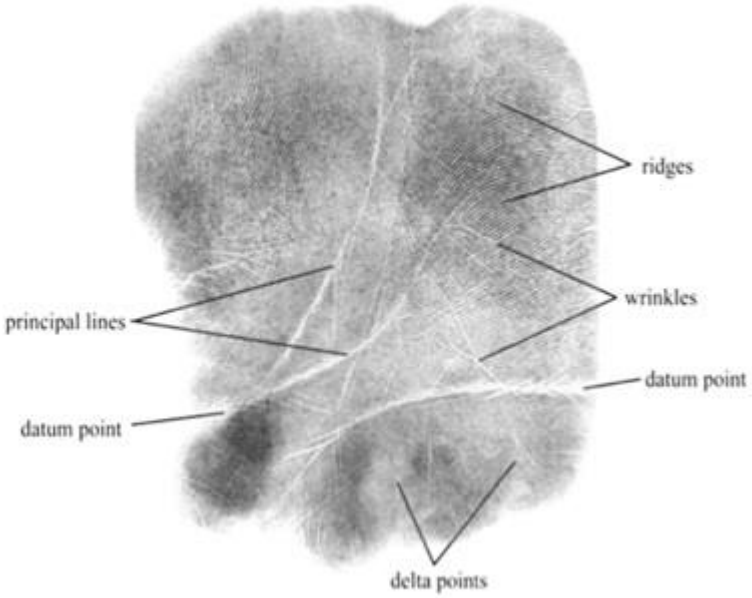

(a)

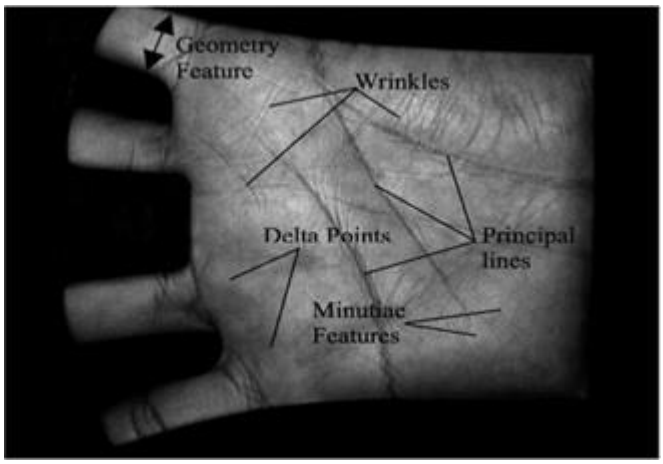

(b)

Figure 3 Different features on a palm (a), inked palmprint, b) inkeless palmprint)

Palmprint are rich in features an example is show in Figure 3. Proper definitions of each aspect are presented.

a. *Geometry features:* Are related geometric structures of the hand. This structure includes width of the fingers at various locations, width of the palm, thickness of the palm, length of the fingers, etc. There are several algorithms in the literature on the hand geometry, combining different features as based on contours or on

geometric features, and so on. Figure 4 Show the features for length, width, and thickness in geometry hand.[11]

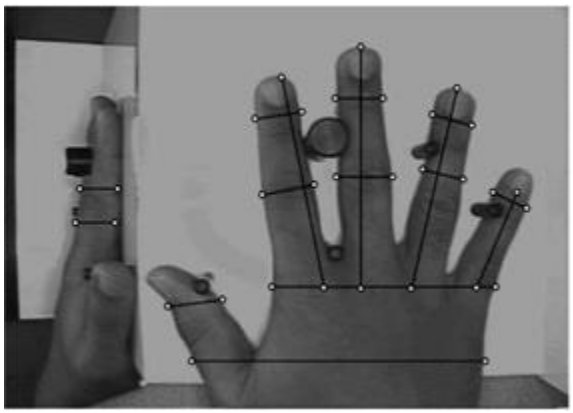

Figure 4 Geometry features on hand

b. *Principal line features:* Is based on the main lines of the hand, taking into account the location and shape of this. Because they vary little in time, these features are commonly used for low-resolution palmprint identification systems [12]. Figure 5. Shows different lines on a hand.

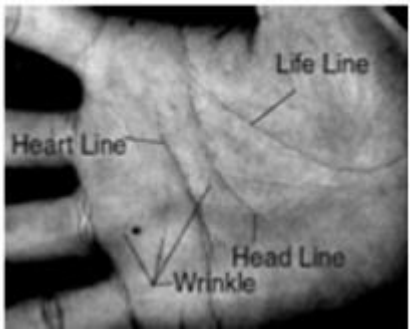

Figure 5 Different lines on a palm

c. *Wrinkle features:* These are the small lines cross the principal lines. The extraction of these lines should be done with a fair precision. This is not an easy task, because these lines are more irregular. Thus wrinkles are not a widely used feature. In Figure 6 shows different wrinkles features.[13]

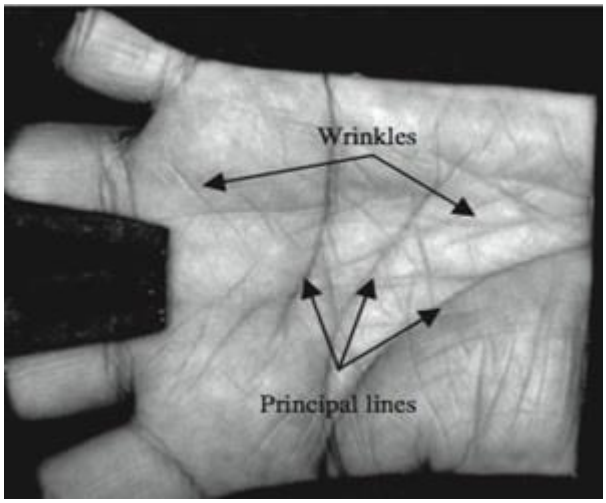

Figure 6 Wrinkles features

d. *Delta point features: Are* defined on the center of a delta-like region in the palmprint. There are delta points located in the finger-root region as well. Figure 7 Shows the delta points in inked palmprint [12].

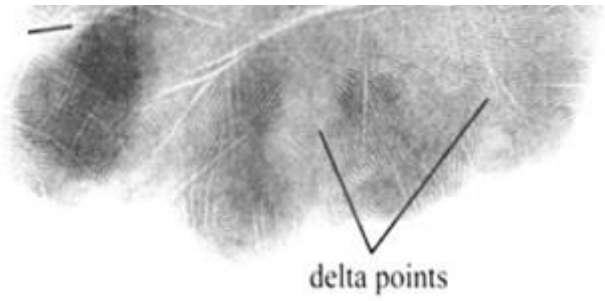

Figure 7 Delta point features

e. *Datum points:* Two end points called datum points are obtained by using the principal lines. These intersect both sides of palm and provide a stable way to register palmprints. Once in a database, the size of palm can be estimated by using the Euclidean distance between these end points Figure 8 shows the datum points in inkeless palmprint [12].

Figure 8 Datum point features

f. *Minutiae features:* Are the principal features used in the fingerprint patterns. A minutia refers to the part or parts of a ridge where an alteration of the trajectory happens [9]. Several types of minutiae can be considered (e.g., termination, bifurcation and dot). Figure 9 different minutiae in a sample palmprint are show.

Figure 9 Different types of minutiae in palmprint

Palmprint authentication requires the comparison of an enrolled sample with another sample taken from a different place. The enrollment has three steps (capture, process, and enroll) followed by a matching step. The matching can be a verification or identification, as mentioned in section 2.1. Figure 10 Show the process for custom palmprint identification (image acquisition, image preprocessing, and feature extraction and matching). For each stage there are different methods, which can be applied on the next section some of them will be described.

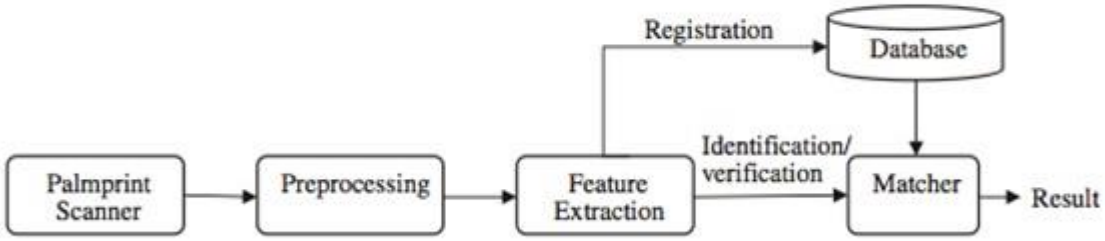

Figure 10 Typical palmprint recognition systems

2.2.1. Palmprint image Acquisition

The first stage occurs when a physical or behavioral sample is inserted into the system. Different devices have been created throughout history and depending on the desired resolution (high or low), measured in dots per inch (pdi), different features can be captured. High-resolution images are suitable for forensic applications such as criminal detection. We can look out for features such as singular point, minutiae and ridges, which refers to 400 dpi or more. Low-resolution images are more suitable for civil and commercial applications such as access control. We can appreciate the hand's geometry or identify wrinkles, principal lines and texture, which refers to 150 dpi or less [13].

Palmprint research employs two main focuses on the palmprint data: offline and online palmprints. For the first, the acquisition of the palmprint data is not directly input to the computer. Instead, it is first inked on a sheet of paper, and then a scanner is used to digitize the data to store it in a computer for further processing. This collection method is very slow; it is not suitable for real time applications. For the second, the acquisition is the most direct way to digitize palmprint data, obviating the need of a third medium like paper. Using a scanner on a palmprint directly, or using a video camera to obtain the palmprint data can accomplish this [12],[14],[15]. This digital method captures high quality palmprint images and aligns palms accurately because the scanners have pegs for guiding the placement of hands [13]

An additional method to comment 3D palmprint recognition, a research done by Zhang et al [16] using mean curvature, Gaussian curvature, and surface type features. Compared with a 2D palmprint image, 3D depth information is difficult to be imitated or disclosed,

thus 3D palmprint recognition is more robust against fake palmprint attacks than 2D palmprint recognition. Since 2D information can also be acquired during 3D reconstruction, a high accuracy and robust palmprint recognition system could be constructed by combining 2D and 3D information [17].

2.2.2. Image Preprocessing

The next step after acquisition is the "preprocessing." The principal goal is to obtain a sub palmprint image for feature extraction and to eliminate the variation caused by the rotation and translation of the original image [18],[19] Preprocessing involves five common steps: 1) Binarizing the palm image, 2) Extracting the contour of hand and/or fingers, 3) Detecting the key points, 4) Establishing a coordinate system and, 5) Extracting the central part [17].

One method used for image preprocessing is Datum Point Registration for online images, exposed first by Zhang and Shu [12]. The idea is to locate two endpoints ***a*** and ***b*** on the edges of the principal lines, which intersect both sides of a palm. Since principal lines are stable, the end points and their mid points remain stable as well. According to the given regularity, the principal lines and their endpoints are accurately detected by using the directional projection algorithm. Experiments with this method obtained great acceptance for palmprint alignment Figure 11 Show de point a and b [12]

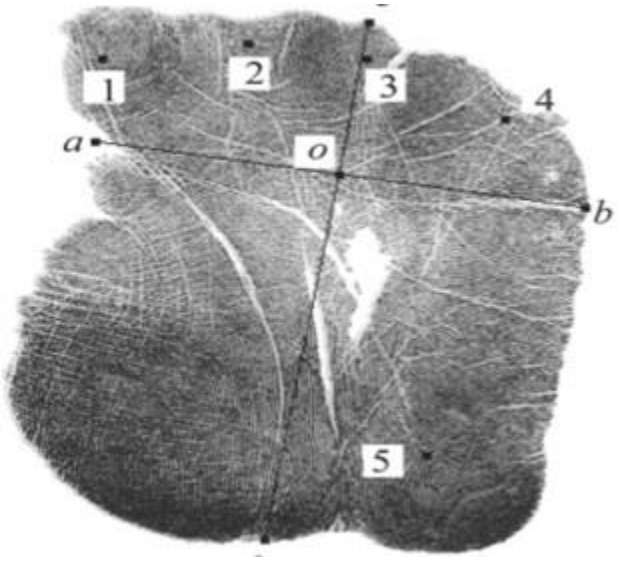

Figure 11 Datum point a, b- endpoints

Another method implemented in [12] is Inked Image in offline images. This method uses two invariant characteristics of palmprint to handle the palmprints with rotation and translation. The experiments based on this alignment method, demonstrated a rate of up to 13% correct identification improvement.

Zhang [12] proposed the palmprint image adaptive threshold algorithm; boundary tracking and automatic positioning palm ROI by Euclidean distance, which guarantees the accuracy and efficiency of the identification system. This approach has many advantages such as a non-complicated algorithm, accurate positioning which can reduce the impact of translation and rotation, high noise endurance and good robustness.[17]

2.2.3. Feature Extraction

The feature extraction is the step where the characteristics of palmprint can be isolated for matching. The features defined posses the stable and unique properties of low intra-class difference and high inter-class difference. Many features of a palmprint can be used to uniquely identify a person, referred in section 2.2. Feature extraction for low-resolution palmprint recognition approaches can be broadly classified into three categories: Holistic-based, feature-based, and hybrid methods.

a) *Holistic-based approach:* Using the original palmprint image as a whole to extract holistic features. There are two main issues for it holistic palmprint image representation and classifier design. Existing several approaches are show in Table 1.

Approach	Representative Work
1. Holistic feature extraction	
1.1 Subspace method	
Unsupervised linear method	Applications of PCA Lu et al [20], Ribaric and Fratric [21]; ICA for Connie et al. [22] Other method for Yang et al. [23]
Supervised linear method	PCA + LDA on raw data for Wu et al. [24]
Kernel method	Applications of kernel PCA for Ekinci and Aykut [25] Kernel Fisher discrimination for Wang and Ruan [26]
Tensor subspace method	Two-dimensional PCA for Zuo et al. [27] Two-dimensional LPP for Hu et al. [28]
Transform domain subspace method	Subspace methods in the transform domains for Jing and Zhang [29]; Jing et al. [30]
1.2 Invariant moment	Zernike moments for Li et al. [31] Hu invariant moments for Noh and Rhee [32]
1.3 Spectral representation	
Wavelet signature	Global statistical signatures in wavelet domain for Zhang and Zhang [33]
Correlation filter	Advanced correlation filter for Hennings et al. [34]; Hennings-Yeomans et al. [34]

Table 1 Approach Holistic features extraction

b) *Feature-based approach:* The visible characteristics of palmprint image are extracted for efficient palmprint recognition. The palm lines and texture are just two classes of many stable and distinctive local features on a human palm. In this approach different features are used, as were described on section 2.2.

Table 2 shows the evaluation of features in terms of acquisition, resolution, collectability, permanence, distinctiveness, circumvention, and application in latent recognition.[17].

Feature	Resolution	Collectability	Permanence	Distinctiveness	Circumvention	Latente Recognition
Principal Lines	Low	High	High	Low	High	No
Wrinkles	Median	High	Median	High	High	No
Multispectral	Low	Median	High	High	Low	No
3D	Median	Low	Median	Median	Median	No
Minutiae	High	Median	High	High	Median	Yes
Level 3	Very High	Low	Median	High	Low	Yes

Table 2 List of features in local features palmprint

Not all features have high levels in all the categories and not every feature is usable. Moreover, **Table 3**, shows different line-based approach for feature extraction and different representative works for each approach are briefly explained [17]

Approach	Representative work
1. Linea-based	
Derivatives of a Gaussian	First and second order derivatives of a Gaussian with different directions for Wu et al [36]
Wide line detector	Extraction of the location and width information of palm line for Liu et al [37]
Line segment Hausdorff distance	Application of line segment Hausdorff distance for Gao and Leung [38]
2. Coding-based	
PalmCode	Coding of the phase of the 2D-Gabor filter responses for Zhang et al [39]
FusionCode	Coding of the phase of the 2D-Gabor filter responses with the maximum magnitude for Kong et al. [40]
Orientation Code	Coding of the orientation information of palm lines for Jia et al. [41]; Kong and Zhang et al. [42]; Sun et al. [43].
3. Palmprint texture description	Local binary patterns for Wang et al. [44] Coding DTC coefficients, Kumar and Zhang [45]

Table 3 Line-based approaches

c) *Hybrid approach:* Use both holistic and local features to improve the recognition accuracy matching speed. The combination and accumulation of several features is reflected in higher accuracy for the matching. In this have two approaches, multiple palmprint representation and Hierarchical matching schema. In the first the representative work is of Kumar and Zhang [46] is Fusion of three palmprint representation, Gabor, Line and subspace features. On second approach the representative work is of Li et al. [47]; and You et al. [48] if Coarse-to-fine matching of palmprint representation Multiple The disadvantage of these approach is in the increase of computational resources and the complexity of developing, involving a high economic cost, and thus a difficult implementation[17].

2.2.4. Feature Matching /Classification Methods

In the end of the process is feature matching. In this step the correspondence between the features detected in the sensed image and those detected in the reference image is established [12]. To make the comparison of palmprint images can be obtained two types of responses, which are [49]:

- *Both palmprints are similiar according to scale (0 and 1):* in this case we can represent two options: The first case represents a probability in which **1** means that the two-palmprint images are completely equal and **0** completely different. In the second case, represents a distance, where **0** indicates that they are completely identical and **1** is completely different.

- *A binary decision (Match / Non-match):* In this case the comparison algorithms have a threshold, which is compared with the output of the algorithm, where if the output is above the threshold is decided that the palmprint are equal, the contrary is decided to be different.

When comparing two palmprints **T** and **I**, where **T** the representation of the palmprint register temple on the system and **I** represent a new input image in de system. The

matching is a very difficult problem, mainly due to the large variability in different imprecisions of the same palmprint. The main factors responsible for the variability are summarized below [10]:

- *Displacement*: The same palmprint may be placed at different locations on a touch sensor during different acquisitions resulting in a (global) translation of the palmprint area.
- *Rotation*: the same palm may be rotated at different angles with respect to the sensor surface during different acquisitions.
- *Partial overlap:* palm displacement and rotation often cause part of the palmprint area to fall outside the sensor's "field of view," resulting in a smaller overlap between the foreground areas of the template and the input palmprints.
- Non-linear distortion: the act of sensing maps the three-dimensional shape of a palm onto the two-dimensional surface of the sensor. This mapping results in a non-linear distortion in successive acquisitions of the same palm due to skin plasticity.
- *Pressure and skin condition:* the ridge structure of a palm would be accurately captured if ridges of the part of the palm being imaged were in uniform contact with the sensor surface.
- *Noise:* the palmprints sensing system mainly introduces it; for example, residues are left over on the glass platen from the previous palmprints capture.
- *Feature extraction errors:* the feature extraction algorithms are imperfect and often introduce measure.

For applications, this variability is even higher than the one in more ideal applications like door sensors or live identification. Since the matching algorithm depends on the image resolution, different approaches can be used [49]:

A. Low resolution approach based image correlation

Two palmprint images are superimposed and the correlation between the corresponding pixels is computed for different alignments. One method described

in [49] is summarized below:

The palmprints images T and I, to calculate the diversity of both images the measure is the sum of squared differences (SSD) between the intensities [10]:

$$\boldsymbol{SSD(T,I) = ||T-I||^2 = (T-I)^t(T-I) = ||T||^2 + ||I||^2 - 2T^tI} \qquad \textbf{(1)}$$

Where the super index "**t**" is the transposition of the matrix. The terms $||\mathrm{T}||^2$ and $||\mathrm{I}||^2$ are constant and independents the correlation between two images. The diversity between two images is minimized when the cross-correlation ***(CC)***, $\boldsymbol{CC(T,I) = T^t}$, between $\boldsymbol{T}$ and $\boldsymbol{I}$ is maximized.

Since the term "$\boldsymbol{T^t, I,}$" appears in a negative way to the function of the density, then we can say that it is a function that represents the similarity between images. However, due to the possible displacement and rotation that inevitably appears when you place your palmprint on the sensor, if similarity between images cannot be calculated directly overlaying both images and applying the CC function.

Let $\mathbf{I}^{(\Delta x,\Delta y,\theta)}$ represent a rotation of the input image $\mathbf{I}$ by an angle $\boldsymbol{\theta}$ around the origin and shifted by $\boldsymbol{\Delta x}$ and $\boldsymbol{\Delta y}$ pixels in directions $\boldsymbol{x}$ and $\boldsymbol{y}$, respectively. If $\boldsymbol{I'^{(\Delta x,\Delta y,\theta)}}$ is the image vectorized of $\boldsymbol{I^{(\Delta x,\Delta y,\theta)}}$. Then, the simalirity in both images can be measure for:

$$\mathbf{S(T,I) = \max_{\Delta x,\Delta y,\theta} CC(T', I'^{(\Delta x,\Delta y,\theta)})} \qquad \textbf{(2)}$$

The direct application of this equation rarely provides acceptable results due to variability problems already discussed. This equation only takes into account the rotation and movement of the palmprint but does not consider all the other factors of distortion or variability. In addition, the direct computation of this equation is very expensive.

B. Low resolution approach based principal lines

In general this approach the object of matching is to tell whether two line

segments from a couple of palmpints images are the same in a palmprint. In some algorithms such as the stack filter [50], can obtain these lines. However, the principal lines do not contribute adequately to high accuracy because of their similarity amongst different palms. So, wrinkles play an important role in the low-resolution palmprint identification, however the accurately extracting wrinkles are still a difficult task, for this reason to apply texture analysis to palmprint [12].

C. High resolution approach based minutiae

Previously the low-resolution palmprint recognition is based on encoding and matching creases, which are less reliable then ridges. Traditionally, ridges have been studied for fingerprint matching techniques, however three main advantages can be found on analyzing ridge patterns on palmprint rather then fingerprints, mentioned in section 2.1. The matching process with minutiae is explaining a continuously [10]:

Given two images of a **T** template and an input image **I**, a minutiae extraction process is executed to extract a set of minutiae of the form:

$$\boldsymbol{T} = \{\boldsymbol{m_1}, \boldsymbol{m_2}, \ldots \boldsymbol{m_m}\}, \boldsymbol{m_i} = \{\boldsymbol{x_i}, \boldsymbol{y_i}, \boldsymbol{\theta_i}, \boldsymbol{t_i}\}, \boldsymbol{i} = \boldsymbol{1} \ldots \boldsymbol{m} \quad \textbf{(3)}$$

$$\boldsymbol{I} = \{\boldsymbol{m'_1}, \boldsymbol{m'_2}, \ldots \boldsymbol{m'_m}\}, \boldsymbol{m'_j} = \{\boldsymbol{x'_j}, \boldsymbol{y'_j}, \boldsymbol{\theta'_j}, \boldsymbol{t'_j}\}, \boldsymbol{j} = \boldsymbol{1} \ldots \boldsymbol{n} \quad \textbf{(4)}$$

Where:

- $\boldsymbol{m}$ and $\boldsymbol{n}$, represent the number of minutiae in sets of $\boldsymbol{T}$ and $\boldsymbol{I}$
- $\boldsymbol{x}$ and $\boldsymbol{y}$, represent the position of the minutiae in the image.
- $\boldsymbol{\theta}$, Represent the orientation (angle) of the minutiae
- $\boldsymbol{t}$, Represent the type of the minutiae, where ***t ϵ {temination, bifurcation}***

Will considered a minutia $\boldsymbol{m'_j}$ in **I** and a minutia $\boldsymbol{m_i}$ **in T** are considered "matching", if the spatial distance (SD) between them is smaller than tolerance threshold $\boldsymbol{r_0}$ and the direction difference (dd) between them is smaller than an angular tolerance threshold $\boldsymbol{\theta_0}$. This threshold is necessary to compensate for the

unavoidable error made by feature extraction algorithms.

The other hand, two minutiae are matching if following the condition is met:

$$\boldsymbol{sd}(\boldsymbol{m'_j}, \boldsymbol{m_i}) = \sqrt{(\boldsymbol{x'_j} - \boldsymbol{x_i})^2 + (\boldsymbol{y'_j} - \boldsymbol{y_i})^2} \leq \boldsymbol{r_0} \qquad \textit{(5)}$$

$$\boldsymbol{dd}(\boldsymbol{m'_j}, \boldsymbol{m_i}) = \boldsymbol{min}(|\boldsymbol{\theta'_j} - \boldsymbol{\theta_i}|, \boldsymbol{360^\circ} - |\boldsymbol{\theta'_j} - \boldsymbol{\theta_i}|) \leq \boldsymbol{\theta_0} \quad \textit{(6)}$$

Where the function ***dd*** takes only the minimum between $|\boldsymbol{\theta'_j} - \boldsymbol{\theta_i}| \; \boldsymbol{and} \; \boldsymbol{2\pi} - |\boldsymbol{\theta'_j} - \boldsymbol{\theta_i}|$ in order to consider the circularuty of an angle. Else, case where, for example $\theta'_j = 355°$ and $\theta_i = 10°$ will deduct a $dd = 345°$ instead of $dd = 15°$

One step important for maximize the number of matching minutiae is the aligning the two palmprints. Correctly aligning two fingerprints certainly requires displacement in $\Delta x \; and \; \Delta y$ and rotation in θ to be recovered. To defined ***map()*** with the function that maps a minutia $\boldsymbol{m'_j}$ into $\boldsymbol{m''_j}$ according to a given geometrical transformation, where a new set I'', and formed so for:

$$\boldsymbol{map}_{\Delta x, \Delta y \Delta, \theta}(\boldsymbol{m'_j}) = \boldsymbol{m''_j} \quad \textbf{(8)}$$

where

$$\boldsymbol{m''_j} = \{\boldsymbol{x''_j}, \boldsymbol{y''_j}, \boldsymbol{\theta''_j} \boldsymbol{t''_j}\} \quad \textbf{(9)}$$

To calculate the new position and angle are:

$$\boldsymbol{\theta''_j} = \boldsymbol{\theta'_j} + \boldsymbol{\theta}$$

$$\begin{bmatrix} \mathbf{x''_j} \\ \mathbf{y''_j} \end{bmatrix} = \begin{bmatrix} \mathbf{cos\theta} - & \mathbf{sin\theta} \\ \mathbf{sin\theta} & \mathbf{cos\theta} \end{bmatrix} \begin{bmatrix} \mathbf{x'_j} \\ \mathbf{y'_j} \end{bmatrix} + \begin{bmatrix} \mathbf{\Delta x} \\ \mathbf{\Delta y} \end{bmatrix} \qquad \textbf{(10)}$$

And finally, we will define the function mm(), be an indicator that return 1 in the case where the minutiae m''_j and m_i match, so that, for every possible combination:

$$\mathbf{mm}(\mathbf{m''_j}, \mathbf{m_i}) = \begin{Bmatrix} \mathbf{1 \; sd}(\mathbf{m''_j}, \mathbf{m_i}) \leq \mathbf{r_0 \; and \; dd}(\mathbf{m''_j}, \mathbf{m_i}) \leq \mathbf{\theta_0 \; and \; t''_j = t'_i} \\ \mathbf{0 \; otherwise} \end{Bmatrix} \textbf{(11)}$$

Then, this problem can be formulated as:

$$\boldsymbol{max}_{\Delta x,\Delta y,\theta,P} \sum_{i=1}^{m} \boldsymbol{mm}\left(\boldsymbol{map}_{\Delta x,\Delta y,\theta}\left(\boldsymbol{m'}_{P(i)}\right), \boldsymbol{m}_i\right) \quad \textbf{(12)}$$

Where P(i) is an unknown function that determines the pairing between ***I*** and ***T*** minutiae.

One method by Ratha et al in 1996 [51], proposed a generalized Hough transform-based minutiae matching, whose underlying alignment transformation, besides displacement and rotation, also includes scale. The space of transformations consists of quadruple $(\boldsymbol{\Delta x}, \boldsymbol{\Delta y}, \boldsymbol{\theta})$, where each parameter is discretized into a finite set of values:

$$\boldsymbol{\Delta_x^+ \epsilon}\left\{\Delta_{\mathbf{x_1}}^+, \Delta_{\mathbf{x_2}}^+, \ldots \Delta_{\mathbf{x_2}}^+\right\}, \quad \boldsymbol{\Delta_y^+ \epsilon}\left\{\Delta_{\mathbf{y_1}}^+, \Delta_{\mathbf{y_2}}^+, \ldots \Delta_{\mathbf{y_2}}^+\right\}, \quad \boldsymbol{\theta^+ \epsilon}\{\boldsymbol{\theta_1^+}, \boldsymbol{\theta_2^+}, \ldots \boldsymbol{\theta_b^+}\} \quad (\mathbf{14})$$

With this discretization, a three-dimensional matrix is defined **A** where each axis is one of the three parameters of transformation and where each cell is a possible combination of these values discretely**,** $\boldsymbol{A[\Delta_x^+, \Delta_y^+, \theta^+]}$.

Then the algorithm is shown:

for each $\mathbf{m}_i$, $i = 1 \ldots m$
for each $\mathbf{m}'_j$, $j = 1 \ldots n$
  for each $\theta^+ \in \left\{\theta_1^+, \theta_2^+, \ldots \theta_c^+\right\}$
    if $dd\left(\theta'_j + \theta^+, \theta_i\right) < \theta_0$

$$\left\{\begin{bmatrix}\Delta x \\ \Delta y\end{bmatrix} = \begin{bmatrix}x_i \\ y_i\end{bmatrix} \cdot \begin{bmatrix}\cos\theta^+ & -\sin\theta^+ \\ \sin\theta^+ & \cos\theta^+\end{bmatrix} \begin{bmatrix}x'_j \\ y'_j\end{bmatrix}\right.$$

$\Delta x^+, \Delta y^+$ = quantization of $\Delta x, \Delta y$ to the nearest bin
$\mathbf{A}[\Delta x^+, \Delta y^+, \theta^+] = \mathbf{A}[\Delta x^+, \Delta y^+, \theta^+] + 1\}$

Figure 12 Algorithm generalized Hough transform-based

And the end of the accumulation process, the best alignment transformation $\left(\boldsymbol{\Delta_x^+}, \boldsymbol{\Delta_y^+}, \boldsymbol{\theta^+}\right)$, is obtained as:

$$\left(\boldsymbol{\Delta_x^+}, \boldsymbol{\Delta_y^+}, \boldsymbol{\theta^+}\right) = \mathbf{arg\,max}_{\boldsymbol{\Delta_x^+}, \boldsymbol{\Delta_y^+}, \boldsymbol{\theta^+}} \mathbf{A}[\boldsymbol{\Delta_x^+}, \boldsymbol{\Delta_y^+}, \boldsymbol{\theta^+}]. \quad \textbf{(15)}$$

In this algorithm the number of elements in the discretized displacement, and in the angle, b, depends on the application. The larger, slower is the algorithm. In addition, if is discretized into many values, we found that all samples fall mostly in different discrete values and then the algorithm does not work. This algorithm is no good for partial to full comparisons, since the alignment is made with one piece of image versus the whole counterpart, and a lot of time wasted.

Others methods have been presented for palmprint recognition of high – Resolution. In Table 4 show different approaches [52]:

Algorithm	Accuracy and efficiency
Jain and Demirkus[53]	The methods are based in minutiae point and SIFT points. The alignment the heart line used for full palmprint. The matching is partial-to-full images, with de identification rate is 96%, but is extremely slow in computation.
Jain and Feng[54]	The method is based in minutiae points and orientation field. The Alignment rigid base don most similar minutiae pairs. The matching is Latent-to-full images, with identification rate is 69% and the Partial-to-full is 78.7%, but is slow in computation.
Dai and Zhou[55]	The method is based in minutiae points, ridge density, map, principal map, and orientation field. The alignment is Rigid using Hough transform. The matching is Partial-to-full, with intensification rate 91,7%, but is very slow in computation.

Dai et al. [56]	The method is based in minutiae points, orientation field and ridge density map. The alignment is the average orientation field for coarse full palmprint and generalized Hough transform for fine segment level alignment, manual alignment for partial palmprints. The matching is Partial-to-full, with the rate is 91,9% and 97,9 in full-to-full images. In the computation is very good.
Capelli et al [57]	The method is based in minutiae Cylinder Code (MCC). The matching is Full-to-full and error is less than 0,01% . The computation is very robust.
Liu et al [52]	The method is based in minutiae points, orientation descriptor and ridge period descriptor. The alignment propagation from initial minutiae pairs. The matching is Latent-to-ful, with identification rate is 79,4%. The computation is very robust.

Table 4 Matching Approach Minutiae based

However, it is again unclear if the method works for partial palmprints and, since it is based more features than the minutiae, requires a higher definition and quality than images found on. In general of this algorithms is that this decomposition is very sensitive to the length of the obtained palmprint and again, cannot be used to satisfy partial to full matching requirements.

2.3. Justification for new Matching Algorithm

In the forensic palmprint it is more usual to detect a tiny partial image rather a full sample and the most palmprint matching approach are based on a full-to-full association, our contribution is based in tiny section of the palmprint being association with its complete counterpart. Only the method present in [54] considered this fact although they need a larger palmprint our requirements.

CHAPTER III

3. PARTIAL TO FULL IMAGE REGISTRATION

Consider we want to align a small image to a large image. We suppose the small one shows part of the larger one. For this reason, we say the small image is a partial image $\boldsymbol{P}$ and the larger one is a full Image $\boldsymbol{F}$. Both images are represented by their salient points, $(\boldsymbol{x^P}, \boldsymbol{y^P}) = \{(\boldsymbol{x_1^P}, \boldsymbol{y_1^P}),\ \dots, (\boldsymbol{x_{|P|}^P}, \boldsymbol{y_{|P|}^P})\}$ and $(\boldsymbol{x^F}, \boldsymbol{y^F}) = \{(\boldsymbol{x_1^F}, \boldsymbol{y_1^F}),\ \dots, (\boldsymbol{x_{|F|}^F}, \boldsymbol{y_{|F|}^F})\}$ together with their features $\mathbf{f^P} = \{\mathbf{f_1^P}, \dots, \mathbf{f_{|P|}^P}\}$ **and** $\mathbf{f^F} = \{\mathbf{f_1^F}, \dots, \mathbf{f_{|F|}^F}\}$. The number of salient points is $|\boldsymbol{P}|$ and $|\boldsymbol{F}|$**,** respectively.

Our algorithm has two main steps. Figure 13 Shows the step and the next explain this.

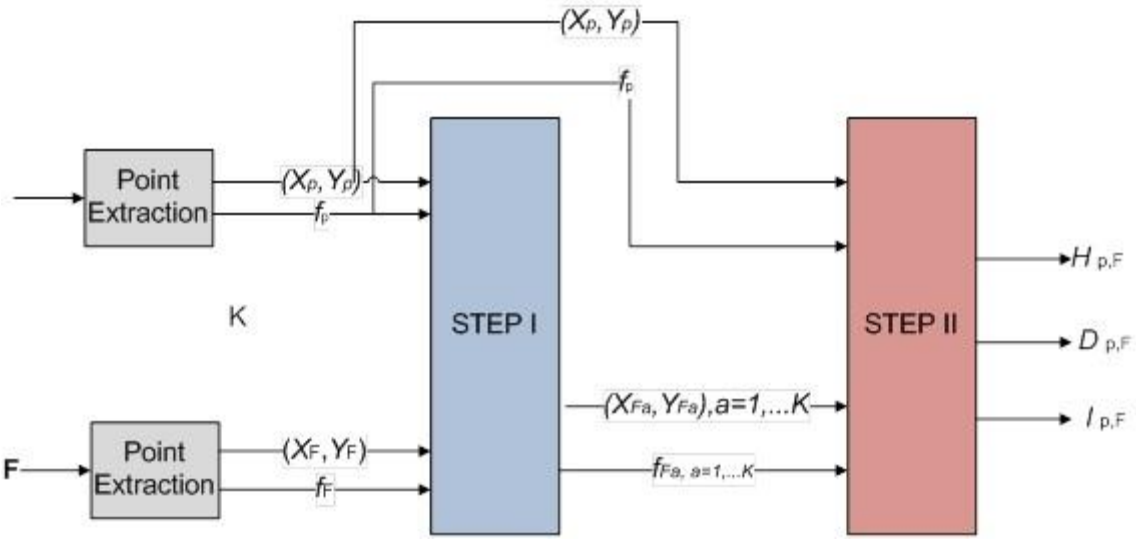

Figure 13 Diagram of the registration method

In the first step, k positions $(\boldsymbol{x_1^c}, \boldsymbol{y_1^c})$,, ... $(\boldsymbol{x_k^c}, \boldsymbol{y_k^c})$ on the full image $\boldsymbol{F}$ are selected as candidates to be the centre of the partial image $\boldsymbol{P}$ if both images were aligned. Then, the full image $\boldsymbol{F}$ is split in some images $\boldsymbol{F_1}, \dots \boldsymbol{F_k}$**,** in which the centre of each image $\boldsymbol{F_a}$ is the candidate position $(\mathrm{x_a^c}, \mathrm{y_a^c})$. Each split image F_a is represented by their set of salient points $(\boldsymbol{x^{F_a}}, \boldsymbol{y^{F_a}}) = \left\{(\boldsymbol{x_1^{F_a}}, \boldsymbol{y_1^{F_a}}),\ \dots, (\boldsymbol{x_{|F_a|}^{F_a}}, \boldsymbol{y_{|F_a|}^{F_a}})\right\}$ and also their corresponding set of

features $\boldsymbol{f^{F_a}} = \left\{\boldsymbol{f_1^{F_a}}, \ldots, \boldsymbol{f_{|F_a|}^{F_a}}\right\}$. Note that the number of extracted salient points in the partial image $|\boldsymbol{P}|$ and the split ones $|\boldsymbol{F_a}|$ can be different. Moreover, $|\boldsymbol{F}| \leq \sum_{a=1}^{k} |\boldsymbol{F_a}|$, since the split images can overlap.

In the second step, the algorithm seeks the best alignment between the salient points $(\boldsymbol{x^P}, \boldsymbol{y^P})$ of the partial image *P* and the salient points $(\boldsymbol{x^{F_a}}, \boldsymbol{y^{F_a}})$ of each of the split images $\mathbf{F_1}, \ldots, \mathbf{F_k}$. To obtain these alignments, not only the salient point positions are used but also their extracted features. More precisely, we use features $\boldsymbol{f^P}$ and $\boldsymbol{f^{F_a}}$. Thus, $\boldsymbol{k}$ distances $\mathbf{D_1}, \ldots, \mathbf{D_k}$ and *k* alignments (also called homographies) $\boldsymbol{H_1}, \ldots, \boldsymbol{H_k}$ are computed. Finally, the method selects the image that obtains the minimum distance and returns the alignment $\boldsymbol{H_{P,F}}$ between $\boldsymbol{P}$ and $\boldsymbol{F}$ that obtains this distance. We have called our method *Tiny to full*.

3.1. Selecting some position candidates

Figure 14 shows the main structure of the first step of our method. It is based on a Generalized Hough Transform [10], [59], [17] method. As commented in the previous section, we assume the method first obtains $|\boldsymbol{P}|$ and $|\boldsymbol{F}|$ salient points (position and features) of both images and so the inputs of this first step are these sets of points.

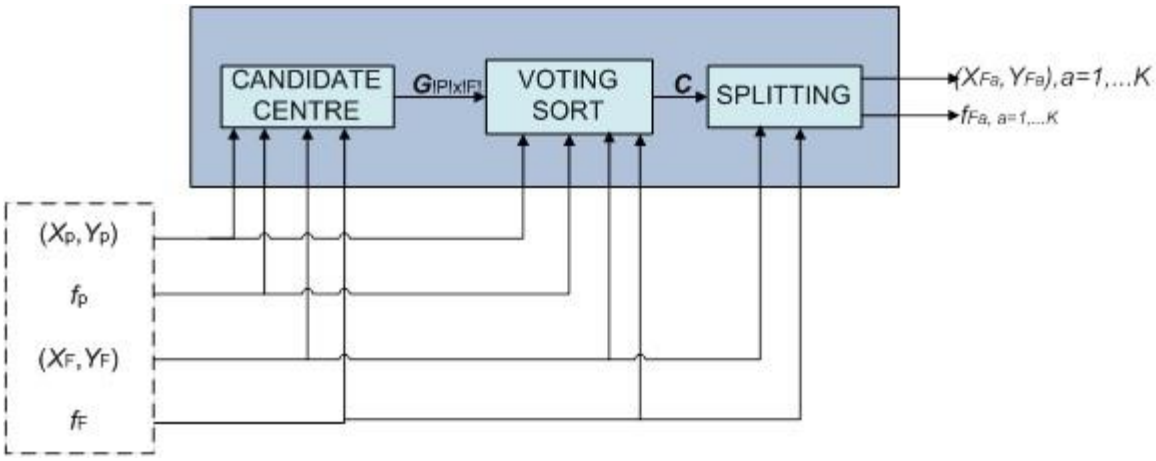

Figure 14 Diagram of step I

We define a $|\boldsymbol{P}|\boldsymbol{x}|\boldsymbol{F}|$ matrix $\mathbf{G}[\mathbf{i},\mathbf{j}]$. The *Candidate Centre* module fills each cell of $\boldsymbol{G}[\boldsymbol{i},\boldsymbol{j}]$ with the position $\left(\boldsymbol{x}_{\boldsymbol{ij}}^{\boldsymbol{C}},\boldsymbol{y}_{\boldsymbol{ij}}^{\boldsymbol{C}}\right)$ on the full image *F* that the centre of the partial image $(\bar{\boldsymbol{x}},\bar{\boldsymbol{y}})$ would obtain if the point $\left(\boldsymbol{x}_{\boldsymbol{i}}^{\boldsymbol{P}},\boldsymbol{y}_{\boldsymbol{i}}^{\boldsymbol{P}}\right)$ on the partial image where mapped to the point $\left(\boldsymbol{x}_{\boldsymbol{j}}^{\boldsymbol{F}},\boldsymbol{y}_{\boldsymbol{j}}^{\boldsymbol{F}}\right)$ on the full image. There are several methods to obtain these centres [17]. They can use only one or several points, and also some information extracted from the features, such as angle information. The aim of this process is to detect the spatial relations on both images. If *s* points in *P* and *s* points in *F* have the same relative position, then there is going to be *s* cells of $\boldsymbol{G}[\boldsymbol{i},\boldsymbol{j}]$ with the same value. These cells are the ones that the mapping between points on both images is the correct one.

When matrix G is filled, then the *Voting and Sort* module generates an ordered list *C* of the positions $\left(\boldsymbol{x}_{\boldsymbol{ij}}^{\boldsymbol{C}},\boldsymbol{y}_{\boldsymbol{ij}}^{\boldsymbol{C}}\right)$ found in $\boldsymbol{G}$, $\boldsymbol{C}=\{(\boldsymbol{x}_{\boldsymbol{1}}^{\boldsymbol{c}},\boldsymbol{y}_{\boldsymbol{1}}^{\boldsymbol{c}}),\ldots,(\boldsymbol{x}_{\boldsymbol{T}}^{\boldsymbol{c}},\boldsymbol{y}_{\boldsymbol{T}}^{\boldsymbol{c}})\}$ through a clustering and voting process. List $\boldsymbol{C}$ is set in a descendent order. This means that, the positions with the most votes are the first ones. Note that $\boldsymbol{T}\leq|\boldsymbol{P}|\boldsymbol{x}|\boldsymbol{F}|$.

The voting process counts the number of centers grouped by the clustering process and also that their features are considered to be similar enough. The clustering process takes into account two center points $\left(\mathbf{x}_{\mathbf{ij}}^{\mathbf{C}},\mathbf{y}_{\mathbf{ij}}^{\mathbf{C}}\right)$ **and** $\left(\mathbf{x}_{\mathbf{i'j'}}^{\mathbf{C}},\mathbf{y}_{\mathbf{i'j'}}^{\mathbf{C}}\right)$, which have to be considered the same if they are close enough. This happens when the distance is lower than a spatial threshold, $\boldsymbol{dist}_{\boldsymbol{P,M}}^{\boldsymbol{position}}\left(\left(\boldsymbol{x}_{\boldsymbol{ij}}^{\boldsymbol{C}},\boldsymbol{y}_{\boldsymbol{ij}}^{\boldsymbol{C}}\right),\left(\boldsymbol{x}_{\boldsymbol{i'j'}}^{\boldsymbol{C}},\boldsymbol{y}_{\boldsymbol{i'j'}}^{\boldsymbol{C}}\right)\right)<\boldsymbol{T}_{\boldsymbol{s}}$.

Thus, the *Voting and Sort* module counts and orders the cells in $\mathbf{G}$ such that $\boldsymbol{dist}_{\boldsymbol{P,M}}^{\boldsymbol{position}}\left(\left(\boldsymbol{x}_{\boldsymbol{ij}}^{\boldsymbol{C}},\boldsymbol{y}_{\boldsymbol{ij}}^{\boldsymbol{C}}\right),\left(\boldsymbol{x}_{\boldsymbol{i'j'}}^{\boldsymbol{C}},\boldsymbol{y}_{\boldsymbol{i'j'}}^{\boldsymbol{C}}\right)\right)<\boldsymbol{T}_{\boldsymbol{s}}$ **and** $\boldsymbol{dist}_{\boldsymbol{P,M}}^{\boldsymbol{feature}}\left(\boldsymbol{f}_{\boldsymbol{I}}^{\boldsymbol{F}},\boldsymbol{f}_{\boldsymbol{j}}^{\boldsymbol{P}}\right)<\boldsymbol{T}_{\boldsymbol{f}}$. Note that both distances are parameterized. In the case of $\boldsymbol{dist}_{\boldsymbol{P,M}}^{\boldsymbol{position}}$, to be independent of the rotation and scale. In the case of $\boldsymbol{dist}_{\boldsymbol{P,M}}^{\boldsymbol{feature}}$, to be independent of some global feature distortions.

Finally, with the best *K* candidates to be the centre of the partial image on the full image, the set of points $(\boldsymbol{x}^{\boldsymbol{F}},\boldsymbol{y}^{\boldsymbol{F}})$ and the set of features $\boldsymbol{f}^{\boldsymbol{F}}$ are split in $\boldsymbol{K}$ point sets $(\mathbf{x}^{\mathbf{F_a}},\mathbf{y}^{\mathbf{F_a}})$,

$\mathbf{1 \leq a \leq K}$ **and K** feature sets $\boldsymbol{f^{F_a}}$**,** $\boldsymbol{1 \leq a \leq K}$**.** Each point in $\left(\boldsymbol{x_i^F}, \boldsymbol{y_i^F}\right)$ is included in the set F_a if $\boldsymbol{dist_{P,M}^{position}}\left(\left(\boldsymbol{x_i^F}, \boldsymbol{y_i^F}\right), \left(\boldsymbol{x_a^C}, \boldsymbol{y_a^C}\right)\right) \leq \boldsymbol{T_r}$**.** The threshold T_r represents the maximum radius of the set, that is, the maximum distance between any point and the centre of the set. Usually, it is determined depending on the radius of the partial set $(\boldsymbol{x^P}, \boldsymbol{y^P})$**.** The set $\boldsymbol{f^{F_a}}$ **i**s defined congruent with the set $(\boldsymbol{x^{F_a}}, \boldsymbol{y^{F_a}})$**.** Parameter *K* is application dependent and it is commonly a value lower than 4.

3.2. Best candidate selection through multiple correspondences

Figure 15 shows the second step of our registration method.

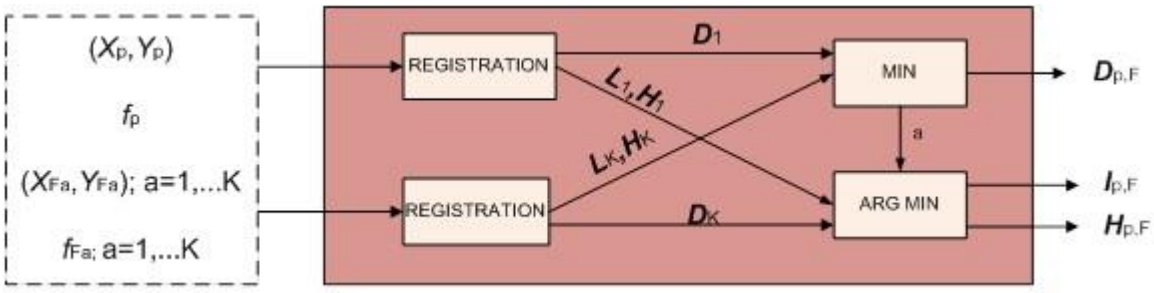

Figure 15 Diagram of step II

In this second step, the method first seeks the distances $\mathbf{D_a = dist(P, F_a);\ 1 \leq a \leq K}$ and the correspondences $\boldsymbol{l_a}$ between the points in each set and also the homographies $\boldsymbol{H_a}$ that transform *P* to $\boldsymbol{F_a}$. Several algorithms can be used to find these correspondences and/or homographies. These algorithms use the positional information $(\boldsymbol{x^{F_a}}, \boldsymbol{y^{F_a}})$ and $(\boldsymbol{x^P}, \boldsymbol{y^P})$ and also their features $\boldsymbol{f^{F_a}}$ and $\boldsymbol{f^P}$**.** For instance the Hungarian method [6] or ICP [5] (when no outliers are considered), RANSAC method [7]. (That considers the presence of outliers), the Bipartite Graph Matching (that considers second order information) and more sophisticated ones [7] or a greedy algorithm that simply selects the best option without considering the other candidates.

We wish to select the set of points $(\boldsymbol{x^{F_a}}, \boldsymbol{y^{F_a}})$ that obtained the minimum distance $\boldsymbol{D_a}$. This is because we assume $\boldsymbol{D_a}$ is a good enough approximation of $\boldsymbol{dist}(\boldsymbol{P}, \boldsymbol{F})$. Moreover, we also assume the correspondence an alignment (homography) between $\boldsymbol{P}$ and $\boldsymbol{F}$ approximates the correspondence $\boldsymbol{l_a}$ and homography $\boldsymbol{H_a}$. Therefore, $\boldsymbol{l_{P,F} = l_a}$ ***and*** $\boldsymbol{H_{P,F} = H_a}$.

Breaking down the full image in a set of candidates has two advantages. On the one hand, the computational cost of obtaining the K distances D_a is lower than obtaining directly the value $\boldsymbol{D_{P,F}}$. On the other hand, the sub-optimal algorithm tends to obtain a more precise local minimum.

CHAPTER IV

4. PRACTICAL VALIDATION

In the practical validation, the only processes throughout our method that has to be defined are the point extractor and the registration process. The rest of the process is independent of the application. On the one hand, we used the minutiae extractor defined in [54], [55], [56] to extract the minutiae from each image. On the other hand, we used the Hough method proposed in [51] as the registration process. The first method, although fingerprint oriented, was considered since it is able to work with few minutiae. The matching algorithm only returns the correspondence between minutiae and the final distance. Moreover, the partial to full palmprint oriented method presented in [60] did not obtained good enough results. Initial experiments showed us that it requires a larger minutiae sample than our aim, for instance a minimum requirement of 150 minutiae.

4.1. Experimental Setup

We have used images contained in the Tsinghua 500 PPI Palmprint Database [60]. It is a public high-resolution palmprint database composed of 500 palmprint images of 2040x2040 resolution and captured with a commercial palmprint scanner from Hisign. From each person, 8 palmprints are enrolled.

We consider four individuals (I). For each individual, 8 palmprint images (PI) are taken into account:

$$\boldsymbol{I_j = \{PI_1, PI_2, \ldots PI_{i.}\}, j = \{1, 2, 3, 4\}\ and\ i = \{1, 2, 3, 4, 5, 6, 7, 8\}.} \quad \textbf{(16)}$$

These palmprints are divided in two sets, the first four palmprints for each individual belong to the reference set T (full palmprint) and the last four belong to test set P (partial palmprint). That is, the full palmprints are kept from the reference set and the partial palmprints are circular patchs given a specific radius (r={100, 200, 300, 400, 500, 600

pixels}, where 100 pixels is equivalent to around 2,5 centimeters) and the center of a palmprint on the test set is random. We obtained an average of 800 minutiae per for palmprint, and from these minutiae the best quality obtained are in the range of 600 and 700 minuteae. Figure 16 shows the subsets ***T*** and ***P*** for one individual.

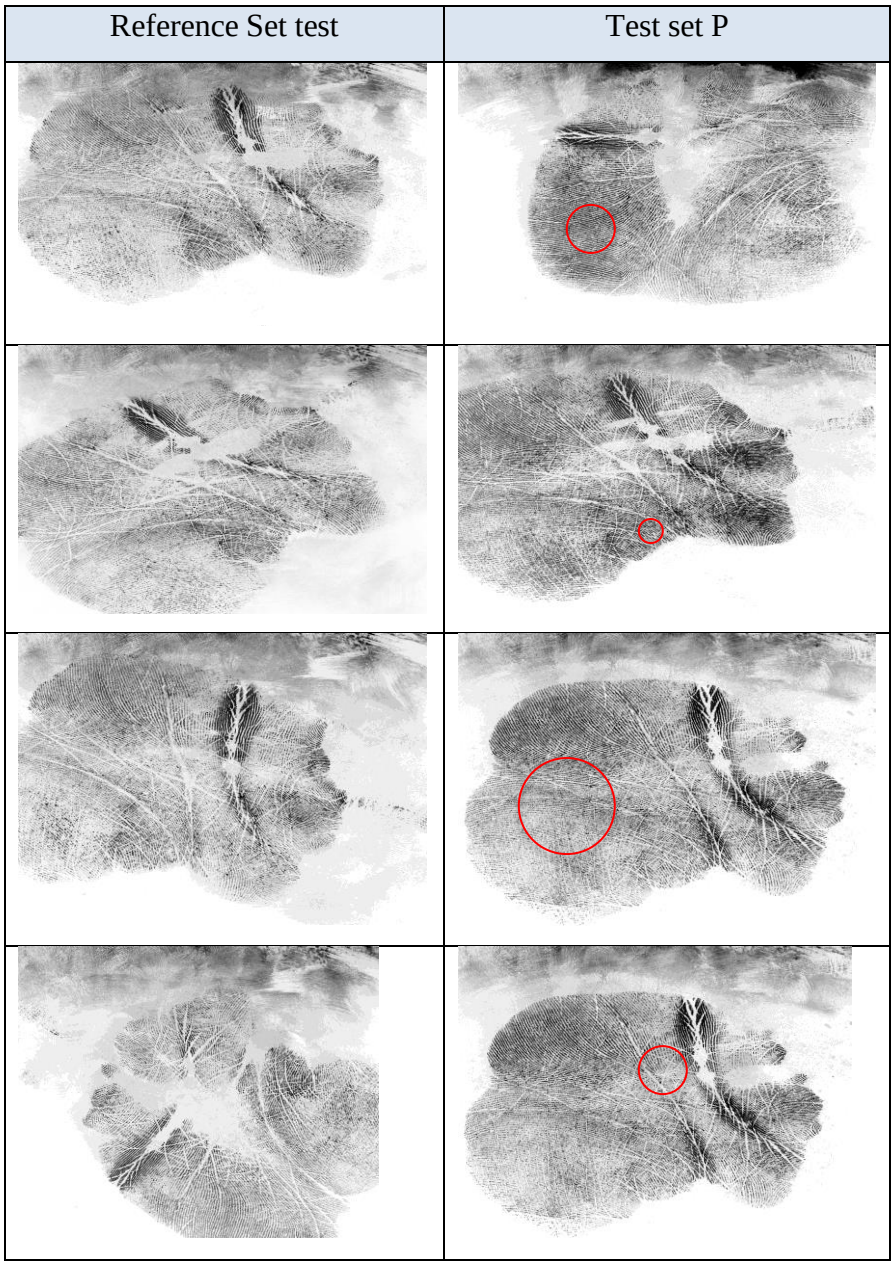

Figure 16 Example reference set (T) and test set (P)

We ran our method with these data. As mentioned in Chapter 3, our method consists of two steps. The first point extractor involves selecting, voting, and splitting candidates

(See Section 3.1). As a result of this step, we obtain the best partial candidate ***(Fa)*** from a full palmprint. The second step (see section 3.2) registration calculates the matching between partial candidate of full palmprint ***(Fa)*** and palmprint on test set ***P***. Figure 17 Show an example of this process.

<table>
<tr><th>Reference Image</th><th>Selected 3 candidates</th><th>Voting- Spliting Best candidate</th><th>Registration</th></tr>
<tr><td>  </td><td>  </td><td> 
(Fa)</td><td rowspan="3">Matching: Calculate distance between Fa and Pj.</td></tr>
<tr><td colspan="3">Test Image</td></tr>
<tr><td>  </td><td colspan="2"> 
Pj</td></tr>
</table>

Figure 17 Example the process our method

4.2. Experiments Results

In Tables 5, 6, 7 and 8 the distances resulted of the matching using our method and Tables 9, 10, 11 and 12 distances resulted of the matching using Hough method between partial palmprints on test set and the partial candidate of the full palmprint in the reference set are shown. Each row represents the selected partial palmprint on the test set ***P***. We applied our method with every image on the reference set. Each column represents the partial candidate of the full palmprint images (**Fa)** on the reference test. The minimum distance for each matching should be contained within the diagonal boxes. However, if this does happen, it is due to errors such as images distorsions. Notice that as ***r*** increases, the tally for correctly identified P increases as well.

Accuracy=6/16			Reference set (T)															
			I1				I2				I3				I4			
			PI5	PI6	PI7	PI8	PI5	PI6	PI7	PI8	PI5	PI6	PI7	PI8	PI5	PI6	PI7	PI8
Test set (P)	(I1)	PI1	6,71	9,21	6,21	6,21	6,71	6,71	8,71	7,71	4,67	4,01	7,00	1,81	3,59	5,01	3,48	5,82
		PI2	2,75	7,45	3,92	4,54	2,70	5,09	3,20	5,22	2,44	3,87	3,88	5,96	3,18	7,22	7,96	10,26
		PI3	5,08	5,08	6,99	5,08	4,39	5,58	6,03	4,59	3,72	4,51	3,49	3,80	9,09	8,16	4,80	4,73
		PI4	1,86	1,86	2,85	4,67	5,53	5,61	4,62	4,94	3,42	5,51	2,85	1,47	7,90	6,54	3,35	1,51
	(I2)	PI1	8,45	6,31	4,40	4,08	6,09	6,65	5,23	2,61	5,12	6,64	5,40	5,15	5,74	6,53	4,22	8,80
		PI2	5,01	5,73	5,59	5,30	7,08	7,47	5,39	3,07	5,47	4,84	4,61	5,17	6,18	7,46	6,66	4,61
		PI3	4,85	5,33	2,83	4,75	8,32	8,32	7,59	4,36	4,16	4,49	5,78	4,11	5,09	6,47	4,02	6,35
		PI4	7,26	7,26	8,23	7,26	3,75	2,45	4,30	4,06	3,49	4,03	3,36	3,49	10,22	4,01	9,72	8,13
	(I3)	PI1	8,25	8,25	7,34	8,25	7,85	8,33	5,69	8,25	3,45	4,02	3,18	5,61	11,30	6,61	4,57	5,99
		PI2	5,40	5,40	5,40	5,40	5,63	5,90	5,54	5,90	3,31	5,09	3,89	4,26	12,12	2,70	3,21	5,11
		PI3	9,22	3,63	3,96	7,80	2,59	2,93	3,12	9,22	7,20	4,08	2,00	4,46	4,61	5,95	5,22	10,13
		PI4	3,35	5,53	1,76	5,60	6,21	3,22	3,61	5,71	2,18	3,88	2,40	5,75	4,55	3,68	6,92	7,00
	(I4)	PI1	6,17	8,48	7,27	7,53	8,69	8,69	8,40	8,25	6,27	3,83	2,45	1,72	10,06	0,95	9,10	7,00
		PI2	4,84	1,88	1,84	6,35	5,72	5,84	5,32	5,32	4,40	3,59	5,43	2,34	10,71	12,79	8,10	9,66
		PI3	8,13	8,13	8,13	8,13	8,10	8,13	7,92	8,13	4,25	7,72	5,19	3,04	4,87	8,51	3,72	8,21
		PI4	3,09	2,42	4,70	4,33	1,48	1,48	8,85	4,00	3,03	2,76	5,74	5,81	9,98	2,91	2,92	8,67

Table 5 Distance of all individual partial palmprints with radius of 100.

Accuracy=7/16			Reference set (T)															
			I1				I2				I3				I4			
			PI5	PI6	PI7	PI8	PI5	PI6	PI7	PI8	PI5	PI6	PI7	PI8	PI5	PI6	PI7	PI8
Test set (P)	(I1)	PI1	18,24	11,10	8,07	20,77	16,92	16,12	9,72	5,88	14,73	9,92	12,07	20,92	8,67	22,86	18,02	26,11
		PI2	20,85	21,65	17,25	18,49	19,78	21,71	17,39	17,64	9,72	11,65	11,25	7,42	15,17	25,28	13,19	20,54
		PI3	18,67	14,66	13,51	17,15	11,62	17,38	10,51	13,04	11,66	13,16	13,58	7,67	29,47	30,26	15,30	17,81
		PI4	20,86	16,94	10,13	19,00	11,33	10,65	12,01	15,22	12,10	15,06	12,31	10,07	31,61	34,49	14,96	22,07
	(I2)	PI1	15,25	12,81	15,21	15,69	15,13	13,56	16,35	10,04	15,52	14,99	18,15	19,28	16,34	18,90	16,04	15,62
		PI2	16,12	9,48	10,91	10,20	13,93	16,85	10,17	10,23	11,19	14,17	10,86	15,68	27,03	27,43	14,32	23,92
		PI3	19,07	19,49	9,08	19,06	19,41	10,13	6,17	10,25	15,61	11,17	10,76	17,63	26,24	32,82	15,59	25,06
		PI4	19,44	20,17	16,88	19,93	9,85	19,88	18,16	10,80	12,57	14,64	17,87	8,43	32,34	20,64	15,53	8,71
	(I3)	PI1	16,19	9,90	11,08	14,50	19,68	22,25	20,56	21,35	11,86	12,58	11,83	11,20	20,37	20,55	13,67	17,81
		PI2	20,59	11,94	15,53	17,50	10,01	12,20	10,94	18,72	14,31	9,23	10,06	14,99	35,83	30,55	10,13	19,07
		PI3	17,15	20,68	21,73	13,49	22,25	27,00	18,83	15,62	10,62	16,14	9,68	8,13	21,47	14,46	16,25	17,03
		PI4	16,56	18,04	9,45	19,88	10,46	20,97	12,82	12,80	12,18	10,92	8,60	13,01	24,47	29,99	15,73	9,63
	(I4)	PI1	19,79	13,36	16,55	20,76	20,07	16,10	14,96	19,76	9,63	17,43	15,00	13,59	23,83	14,28	19,36	4,78
		PI2	15,87	15,56	15,21	16,29	17,06	18,61	10,04	18,00	10,77	12,25	13,15	16,88	18,61	22,88	10,18	14,51
		PI3	9,62	14,34	14,77	17,15	13,94	15,69	17,78	19,13	14,26	9,58	19,74	15,33	19,25	24,86	8,48	25,46
		PI4	14,29	18,59	18,22	21,01	18,54	11,06	13,07	13,72	10,89	10,89	12,92	14,01	18,55	18,65	6,61	8,20

Table 6 Distance of all individual partial palmprint with a radius of 200.

Accuracy= 10/16			Reference set (T)															
			I1				I2				I3				I4			
			PI5	PI6	PI7	PI8	PI5	PI6	PI7	PI8	PI5	PI6	PI7	PI8	PI5	PI6	PI7	PI8
Test set (P)	(I1)	PI1	34,13	52,49	47,43	43,82	45,07	55,00	46,30	49,55	52,26	46,77	48,23	48,56	91,42	85,72	44,22	69,75
		PI2	43,58	48,40	50,13	49,92	50,13	38,22	38,87	47,40	42,68	38,14	40,15	40,20	57,50	96,46	38,13	66,28
		PI3	50,60	50,72	40,12	34,56	34,47	52,97	48,45	47,48	43,45	35,59	46,42	43,99	70,17	74,44	51,04	56,65
		PI4	45,02	26,45	26,06	56,32	40,14	57,44	48,19	39,03	46,32	34,59	36,35	41,34	83,48	91,05	42,67	66,11
	(I2)	PI1	51,67	45,83	53,89	49,31	42,93	52,04	51,95	33,47	50,65	52,40	57,25	57,40	66,32	63,12	45,24	53,31
		PI2	40,58	44,87	38,34	53,00	39,36	41,49	39,78	33,85	42,67	43,51	48,16	51,15	63,56	72,37	34,98	45,94
		PI3	50,97	47,92	47,25	37,04	33,18	31,01	28,51	36,89	39,32	39,50	42,61	47,10	84,19	82,61	52,74	54,25
		PI4	41,97	43,19	42,50	44,72	41,54	33,05	35,63	40,00	36,38	36,94	40,24	45,52	80,09	77,09	43,28	62,29
	(I3)	PI1	46,42	55,33	47,46	44,25	51,85	57,55	50,42	45,20	39,57	52,91	46,05	42,36	76,51	72,98	50,02	52,73
		PI2	47,05	36,02	41,85	44,48	42,67	60,07	45,90	40,55	38,60	39,61	42,74	36,04	83,70	88,63	44,67	43,98
		PI3	51,51	43,40	46,41	44,55	31,36	54,09	40,14	46,91	34,86	35,96	36,43	46,26	43,72	77,78	38,71	59,16
		PI4	44,02	33,35	38,25	58,08	47,68	61,58	43,64	42,47	30,70	31,79	31,42	37,72	78,42	75,60	40,86	34,13
	(I4)	PI1	60,82	52,36	40,15	49,68	31,92	41,37	48,00	57,84	40,46	45,53	55,20	50,18	79,87	32,11	47,63	22,29
		PI2	48,56	50,21	49,85	53,65	43,06	47,68	44,46	47,79	41,64	41,71	52,95	45,30	74,78	88,13	35,27	51,19
		PI3	49,64	46,72	48,93	56,06	42,68	52,90	45,41	41,71	41,07	45,38	50,13	49,90	73,93	33,59	25,01	30,41
		PI4	44,44	47,01	47,23	52,12	42,57	45,91	48,55	41,02	43,55	38,69	37,07	47,24	39,82	39,62	30,86	34,93

Table 7 Distance of all individual partial palmprint with a radius of 400

Accuracy=16/16			Reference set (T)															
			I1				I2				I3				I4			
			PI5	PI6	PI7	PI8	PI5	PI6	PI7	PI8	PI5	PI6	PI7	PI8	PI5	PI6	PI7	PI8
Test set (P)	(I1)	PI1	72,93	71,88	71,44	63,74	68,04	79,27	78,71	97,71	107,10	106,85	109,71	84,93	148,81	123,02	91,72	107,79
		PI2	67,53	65,90	58,59	67,76	72,37	88,62	78,56	94,71	89,04	99,65	92,72	85,85	132,33	148,24	81,20	109,42
		PI3	60,47	58,25	81,21	66,05	66,26	102,13	77,70	102,52	100,06	84,59	96,13	97,55	142,95	138,93	87,70	120,31
		PI4	61,91	61,69	63,87	64,51	63,37	81,76	67,11	102,09	82,64	84,59	99,63	75,06	142,38	107,96	80,96	112,58
	(I2)	PI1	101,28	81,81	111,03	95,68	82,26	83,29	96,90	61,06	109,48	113,78	110,06	111,66	113,70	112,48	86,96	127,04
		PI2	87,63	106,47	103,78	90,62	89,02	87,85	83,36	63,74	98,69	104,71	103,93	96,16	121,43	109,11	82,54	94,71
		PI3	81,97	93,49	86,41	84,00	91,23	77,47	66,03	75,42	101,85	88,94	91,58	83,30	106,94	132,73	97,00	109,22
		PI4	90,79	81,70	81,43	89,41	78,08	78,70	74,89	72,18	91,69	99,26	89,44	104,03	133,04	128,19	82,59	109,34
	(I3)	PI1	89,47	98,19	97,59	97,63	91,73	100,75	97,59	102,08	84,29	90,91	92,01	83,36	115,98	120,22	95,21	88,42
		PI2	88,44	95,72	93,59	105,28	92,19	104,23	95,97	94,23	95,45	85,54	88,75	79,82	115,19	115,92	88,59	95,67
		PI3	106,86	103,12	110,87	109,87	107,37	79,17	98,03	92,96	66,94	70,41	92,89	66,94	124,66	127,32	85,56	81,12
		PI4	89,28	89,42	106,38	101,60	82,32	112,12	108,67	119,06	62,01	70,56	70,65	66,58	112,14	109,32	84,72	81,45
	(I4)	PI1	94,33	86,64	83,29	103,44	92,45	84,14	79,79	113,30	89,52	99,35	81,47	93,94	74,22	75,83	68,26	63,12
		PI2	100,12	84,93	93,05	95,51	100,83	85,86	87,51	100,41	96,38	91,10	115,41	94,76	82,18	81,36	65,49	76,97
		PI3	92,59	85,08	80,69	83,37	97,37	97,19	87,12	101,93	79,21	101,99	92,80	94,60	85,93	86,37	55,34	65,78
		PI4	102,55	90,66	103,49	121,07	104,12	89,72	82,85	86,84	93,17	88,92	88,55	85,46	98,67	91,83	63,41	70,10

Table 8 Distance of all individual partial palmprint with a radius of 600

Accuracy= 4/16			Reference set (T)															
			I1				I2				I3				I4			
			PI5	PI6	PI7	PI8	PI5	PI6	PI7	PI8	PI5	PI6	PI7	PI8	PI5	PI6	PI7	PI8
Test set (P)	(I1)	PI1	295,5	295,5	295,49	295,5	295,5	295,5	295,47	295,5	312,5	312,5	326	326,5	326,5	326,5	326,5	326,5
		PI2	298	298	297,95	298	297,99	298	297,83	298	315	315	328,37	328,98	329	329	329	329
		PI3	300,42	299,81	299,88	300,5	300,5	300,5	300,19	300,5	317,5	317,5	330,98	331,5	331,5	331,5	331,5	331,5
		PI4	296,34	296,17	296,5	296,5	296,5	296,5	296,17	296,5	313,5	313,5	326,94	327,5	327,5	327,5	327,5	327,5
	(I2)	PI1	301	301	300,71	301	300,96	300,84	300,67	301	318	318	331,19	331,79	332	332	332	332
		PI2	300	300	299,22	300	300	299,82	299,66	300	317	317	330,19	330,75	331	331	331	331
		PI3	299,5	299,5	298,78	299,5	299,49	299,17	299,29	299,5	316,5	316,5	329,99	330,5	330,5	330,5	330,5	330,5
		PI4	299	299	298,29	299	297,14	295,19	298,42	299	316	316	328,75	329,91	330	329,38	330	330
	(I3)	PI1	298,5	298,5	298,45	298,5	298,5	298,48	298,45	298,5	315,5	315,5	328,9	329,47	329,5	329,5	329,5	329,5
		PI2	297,5	297,5	297,38	297,5	297,5	297,37	297,46	297,5	314,5	314,5	328	328,5	328,5	328,5	328,5	328,5
		PI3	298	298	297,74	298	298	297,91	298	298	315	315	328,5	329	329	329	329	329
		PI4	297	297,2	297,3	297,5	297,3	297,9	297,4	297,12	314	314	327,5	328	328	328	328	328
	(I4)	PI1	296,5	296,5	296,5	296,5	296,5	296,5	296,44	296,5	313,5	313,5	327	327,25	327,5	327,5	327,5	327,5
		PI2	297	297	297	297	297	297	296,91	297	314	314	327,5	328	328	328	328	328
		PI3	297,5	297,5	297,45	297,5	297,5	297,5	297,37	297,5	314,5	314,5	327,99	328,5	328,5	328,5	328,5	328,5
		PI4	296,5	296,5	296,5	296,5	296,5	296,5	296,45	296,5	313,5	313,5	327	327,5	327,5	327,5	327,5	327,5

Table 9 **Distance of all individual partial palmprint with a radius of 100 Hough**

Accuracy= 5/16			Reference set (T)															
			I1				I2				I3				I4			
			PI5	PI6	PI7	PI8	PI5	PI6	PI7	PI8	PI5	PI6	PI7	PI8	PI5	PI6	PI7	PI8
Test set (P)	(I1)	PI1	302	301,91	299,29	302	299,31	300,39	301,17	300,8	318,83	319	328,33	329,01	333	333	333	333
		PI2	309	308,64	305,68	309	303,03	305,55	304,72	306,26	325,46	325,96	332,51	335,08	340	340	339,84	339,91
		PI3	309	308,67	306,32	309	305,48	306,63	305,82	307,07	325,81	326	333,92	336,19	340	340	340	340
		PI4	309	308,77	306,65	309	305,12	305,62	305,34	307,14	324,36	325,98	334,53	335,45	340	340	339,9	339,96
	(I2)	PI1	318,03	318,97	316,13	319	317	314,95	314,46	313,46	335,46	335,92	342,55	343,82	350	350	349,92	349,92
		PI2	310	309,84	307,56	310	306,97	307,4	306,98	309,01	326,61	326,99	336,58	336,99	341	341	341	341
		PI3	308,5	308,06	303,7	308,5	304,26	303,72	304,49	306,64	325,08	325,49	334,4	335,36	339,5	339,5	339,5	339,5
		PI4	306	305,74	303,52	305,26	304,51	303,77	303	302,95	322,8	323	332,99	333,5	337	335,75	336,95	337
	(I3)	PI1	313,5	313,22	310,25	313,5	308,98	310,31	310,07	311,39	330,24	330,5	340,63	341,04	344,5	344,5	344,5	344,5
		PI2	308,5	307,47	305,22	308,5	305,47	305,54	305,43	307,37	325,25	325,5	336,47	336,86	339,5	339,5	339,5	339,47
		PI3	307,43	306,32	304,85	307,44	304,49	302,99	304,37	306,2	324,14	324,49	334,7	335,23	338,5	338,5	338,38	338,38
		PI4	309	308,8	306,52	309	305,55	307,41	306,24	307,52	325,75	326	335,48	336,66	340	340	339,99	339,96
	(I4)	PI1	304,5	304,5	303,6	304,5	302,4	302,94	301,92	303,9	321,17	321,5	332,24	332,78	335,5	335,5	335,45	335,45
		PI2	308,5	307,7	306,78	308,5	339,45	304,98	304,86	306,74	324,04	325,42	333,32	334,31	339,28	339,5	304,58	339,45
		PI3	307	307	305,76	307	304,53	305,01	304,8	306,15	323,74	324	333,95	333,42	338	338	338	338
		PI4	309	308,68	306,72	309	305,39	305,81	305,4	307,53	325,77	325,96	334,83	335,54	340	340	339,88	340

Table 10 **Distance of all individual partial palmprint with a radius of 200 Hough**

Accuracy= 9/16			Reference set (T)															
			I1				I2				I3				I4			
			PI5	PI6	PI7	PI8	PI5	PI6	PI7	PI8	PI5	PI6	PI7	PI8	PI5	PI6	PI7	PI8
Test set (P)	(I1)	PI1	318,84	311	304,68	317,68	293,52	296,15	294,75	300,5	324,63	325,33	319,43	321,9	349,64	343,97	339,14	338,78
		PI2	333,99	300,47	319,89	332,27	325,96	308,9	305,7	312,16	339,79	339,19	325,4	332,86	365,44	358,93	354,84	355,21
		PI3	334,43	328,05	320,79	332,98	309,76	301,71	308,06	314,89	339,05	338,93	326,07	332,32	365,75	358,51	353,73	353,23
		PI4	334,98	327,86	321,14	333,62	310,98	304,14	308,31	315,4	341,03	341	329,15	334,56	366,42	359,63	356,06	355,55
	(I2)	PI1	361,63	356,46	349,33	361,68	338,84	333,62	336,76	344,36	369,23	370,9	353,67	360,49	393,43	388,74	383,5	380,64
		PI2	343,61	337,34	330,38	343,32	316,92	321,06	312,64	324,72	348,17	349,08	330,87	338,05	374,44	368,11	362,42	360,18
		PI3	334,75	329,25	322,64	333,99	314,25	306,52	310,11	316,93	341,71	342,63	330,53	336,44	366,72	360,61	356,97	355,96
		PI4	337,11	331,47	323,62	336,69	311,18	314,23	307,96	317,87	341,1	342,32	328,73	334,32	367,5	361,82	356,36	353,32
	(I3)	PI1	356,15	347,81	340,68	354,11	329,21	316,5	325,31	332,62	355,29	354,78	335,82	343,3	385,29	376,26	369,47	366,79
		PI2	349,41	342,42	335,24	347,72	349,75	324,21	321,83	328,76	350,36	312,3	335,47	341,65	379,07	370,59	364,76	364,1
		PI3	335,95	327,98	322,5	334,27	312,22	312,59	335,94	317,03	341,72	341,93	328,83	304,56	366,65	360,47	354,94	354,95
		PI4	340,1	332,52	325,82	338,28	318,97	315,27	312,65	306,54	345,09	344,82	330,77	337,97	370,56	363,85	358,87	359,61
	(I4)	PI1	326,73	322	314,75	324,62	310,03	307,89	299,63	312,13	332,44	332,17	329,28	332,24	356,47	349,46	346,68	346,37
		PI2	332,95	327,56	322,68	332,8	355,77	311,8	309,83	316,75	341,96	343,09	330,32	335,88	365,63	360,71	306,37	354,58
		PI3	331,96	325,91	318,29	331,22	312,2	309,94	306,62	299,81	334,81	334,86	325,01	328,7	362,13	354,03	349,41	347,58
		PI4	342,91	337,21	329,81	342,43	362,39	320,79	317,58	324,24	348,12	349,01	333,04	338,65	374,18	367,64	312,13	359,29

Table 11 Distance of all individual partial palmprint with a radius of 400 Hough

Accuracy= 12/16			Reference set (T)															
			I1				I2				I3				I4			
			PI5	PI6	PI7	PI8	PI5	PI6	PI7	PI8	PI5	PI6	PI7	PI8	PI5	PI6	PI7	PI8
Test set (P)	(I1)	PI1	319,06	309,87	293,71	325,63	274,59	286,28	284,45	293,86	303,01	302,7	290,66	295,5	338,82	333,7	311,7	320,46
		PI2	334,17	275,21	302,31	339,03	321,1	293,09	284,7	298,61	310,08	310,01	286,48	291,35	357,3	341,39	321,9	333,59
		PI3	333,39	320,89	274,08	336,22	305,36	293,2	283,03	301,32	306,08	305,34	279,75	288,68	352,91	344,89	316,68	329,33
		PI4	335,8	323,97	307,78	338,27	276,01	295,35	288,2	301,85	313,31	312,54	290,59	298,52	357,68	346,12	324,29	335,27
	(I2)	PI1	363,12	354,4	342,65	368,72	310,02	306,14	317,54	333,68	339,39	339,41	330,25	317,79	378,82	382,72	347,92	344,59
		PI2	357,21	345,07	331,87	357,92	298,56	294,09	309,97	325,47	324,85	325,47	317,93	305,88	367,75	369,19	333,2	333,51
		PI3	341,43	328,57	314,58	344,35	287,07	303,47	295,2	305,56	321,02	321,08	295,89	304,68	358,18	352,78	331,65	337,99
		PI4	342,78	331,82	319,63	344,69	284,26	302,8	297,03	307,35	316,47	317,2	296,51	304,91	352,15	352,78	326,01	331,68
	(I3)	PI1	376,09	363,93	341,71	380,6	300,44	322,64	314,77	325,49	326,07	323,5	298,65	310,06	379,82	370,95	337,79	339,57
		PI2	370,01	357,87	336,22	374,3	298,53	322,33	311	324,93	328,44	326,48	297,79	311,28	379,78	370,83	338,82	344,88
		PI3	346,76	335,59	315,67	355,28	317,86	300,91	295,73	309,25	317,47	283,68	297,77	303,92	366,3	353,11	329,76	337,72
		PI4	360,3	348,28	329,66	365,82	292,33	312,41	306,06	318,2	328,03	328,61	305,34	313,19	378,56	362,64	344,84	351,81
	(I4)	PI1	353,45	346,7	331,68	348,58	296,65	316,5	316,67	322,03	329,08	326,81	316,65	321,5	369,74	358,47	341,85	353,06
		PI2	349,01	338,54	319,81	348,33	321,06	300,66	300,7	304,19	308,94	305,96	300,52	304,22	351,46	340,89	279,77	332,48
		PI3	352,75	342,09	326,06	355,03	353,91	309,48	305,52	313,65	320,01	317,26	300,14	307,23	360,97	287,21	329,65	340,46
		PI4	356,36	345,32	329,94	359,39	335,93	316,36	308,25	322,31	326,7	326,13	298,69	307,63	369,97	365,4	295,46	342,53

Table 12 Distance of all individual partial palmprint with a radius of 600 Hough

In Tables 13, 14, 15 and 16, the confusion matrices corresponding to Tables 5 to Table 8 respectively are show. Given different values of the radius of our method, in these matrices the classification for each individual ***(I)*** and her or his palmprints. Can be seen the confusion matrix shows another perspective of comparing our method. The representation of higher values on the diagonal indicates that the result is optimal. Once again, we consider the columns for the reference set and rows for test set. Notice that the values of the diagonal for our method show a significant improvement.

Confusion Matrix					
		Reference Set (T)			
		I1	I2	I3	I4
Test Set (P)	I1	0	0	4	0
	I2	1	3	0	0
	I3	1	0	2	1
	I4	1	1	1	1

Table 13 Confusion Matrix Radius 100

Confusion Matrix					
		Reference Set (T)			
		I1	I2	I3	I4
Test Set (P)	I1	0	1	3	0
	I2	1	2	1	0
	I3	1	0	3	0
	I4	0	1	0	3

Table 14 Confusion Matrix Radius 200

Confusion Matrix					
		Reference Set (T)			
		I1	I2	I3	I4
Test Set (P)	I1	2	1	0	1
	I2	0	4	0	0
	I3	1	1	2	0
	I4	0	0	0	4

Table 15 Confusion Matrix Radius 400

Confusion Matrix					
		Reference Set (T)			
		I1	I2	I3	I4
Test Set (P)	I1	4	0	0	0
	I2	0	4	0	0
	I3	0	0	4	0
	I4	0	0	0	4

Table 16 Confusion Matrix Radius 600

Additionally, in Table 17, 18, 19 and 20, the confusion matrices corresponding to Tables 9 to Table 12 of Hough Method [56] are show.

Confusion Matrix					
		Reference Set (T)			
		I1	I2	I3	I4
Test Set (P)	I1	2	2	0	0
	I2	2	2	0	0
	I3	3	1	0	0
	I4	0	4	0	0

Table 17 Confusion Matrix Radius 100 pixels Hough

Confusion Matrix					
		Reference Set (T)			
		I1	I2	I3	I4
Test Set (P)	I1	1	3	0	0
	I2	1	3	0	0
	I3	1	3	0	0
	I4	0	3	0	1

Table 18 Confusion Matrix Radius 200 pixels Hough

Confusion Matrix					
		Reference Set (T)			
		I1	I2	I3	I4
Test Set (P)	I1	1	3	0	0
	I2	0	4	0	0
	I3	0	2	2	0
	I4	0	2	0	2

Table 19 Confusion Matrix Radius 400 pixels Hough

Confusion Matrix					
		Reference Set (T)			
		I1	I2	I3	I4
Test Set (P)	I1	2	2	0	0
	I2	0	4	0	0
	I3	0	1	3	0
	I4	0	1	0	3

Table 20 Confusion Matrix Radius 600 pixels Hough

To summarize Figure 18 shows the recognition ratio of Hough Method [56] versus our method with respect to different radius of the partial palmprint. We can conclude that our method has a great acceptance for palmprint samples with small radius, which is ideal for applications in the forensic field. As the radius increases the two methods will tend to have similar result. The recognition rate is simply the total tally for a given radius expressed in (%).

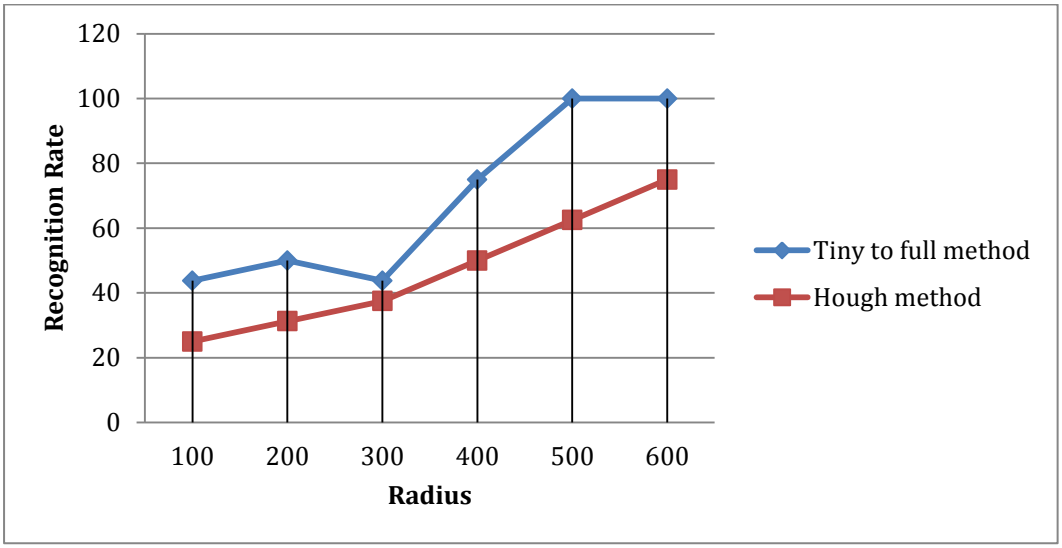

Figure 18 Results of s test comparing method Hough and our method

CHAPTER V

5. CONCLUSIONS

Several algorithms have been presented in the literature to perform palmprint matching. These algorithms need both images to show the full palmprint. These algorithms are useful in a wide range of applications such as verification or identification of people, but they have the important drawback that when the full palmprint is not captured, there is a drastic degradation of the accuracy. In fields such as forensics, it is more usual to detect partial and noisy palmprints. In this case, the usual algorithms suffer from important quality reduction. For this reason, we have presented an algorithm a for partial-to-full palmprint matching. The model has two steps. In the first step, several position candidates are selected and in the second step, only one position is obtained through a multiple assignment method.

In the experimental validation, we showed that it is a useful model because we achieve a higher recognition ratio than a classical method in several dimensions of the partial palmprint.

REFERENCES

[1] Joaquim Salvi, Carles Matabosch, David Fofi, Josep Forest: A review of recent range image registration methods with accuracy evaluation. Image Vision Comput. 25(5): 578-596 (2007).

[2] Barbara Zitová, Jan Flusser: Image registration methods: a survey. Image Vision Comput. 21(11): 977-1000 (2003).

[3] A. Ardeshir Goshtasby, "2-D and 3-D Image Registration for Medical, Remote Sensing, and Industrial Applications", Wiley Press, 2005.

[4] K. Mikolajczyk, C. Schmid, "A performance evaluation of local descriptors", IEEE Trans. Pattern Anal. Mach. Intell. 27 (10), pp: 1615–1630, 2005.

[5] Z. Zhang, "Iterative point matching for registration of free-form curves and surfaces", Int. J. Comput. Vision 13 (2), pp: 119–152, 1994.

[6] Kuhn, H.W.: "The Hungarian method for the assignment problem Export". Naval Research Logistics Quarterly 2(1-2), 83–97 (1955).

[7] M.A. Fischler, R.C. Bolles, "Random sample consensus: a paradigm for model fitting with applications to image analysis and automated cartography", Commun. ACM 24 (6), pp: 381–395, 1981.

[8] Sanromà, R. Alquézar, F. Serratosa & B. Herrera, "Smooth Point-set Registration using Neighbouring Constraints", Pattern Recognition Letters 33, pp: 2029-2037, 2012.

[9] Anil K. Jain, Patrick Flynn, and Arun A.Ross "Handbook of Biometrics", Springer-Verlag, 2008.

[10] Davide Maltoni, Dario Maio, Anil K. Jain and Salil Prabhakar, "Handbook of fingertprint recognition", Springer-Verlag, 2003.

[11] Anil K. Jain, Arun A.Ross and Jain, Patrick Flynn, A prototype Hand Geometry-Based Verification System, 2nd Int'l Conference on Audio- and Video-based Biometric Person Authentication (AVBPA), Washington D.C. 66-171, March 22-24, 1999.

[12] Zhang, D. "Palmprint Authentication". Kluwer Academic Publishers. 2004

[13] Somvanshi, P., Rane, M.. "Survey of Palmprint Recognition". International Journal of Scientific & Engineering Research, 3 (2), 2012

[14] D. Zhang, A. W-K. Kong, J. You, and M Wong. Online Palmprint Identification. IEEE Transactions on Pattern Analysis and Machine Intelligence, 25(9):1041-1050,2003.

[15] Kong, W. K., Zhang, D. "Using Low-Resolution Palmprint Images and Texture Analysis for Personal Identification". ICPR. 2002

[16] ZHANG, D., KANHANGAD, V., LUO, N., AND KUMAR, A. 2010. Robust palmprint verification using 2d and 3d features. *Pattern Recog. 43,* 1, 358–368.

[17] Zhang, D. , Zuo, W., Yue, F., "A Comparative Study of Palmprint Recognition Algorithms", ACM Computing Surveys, Vol. 44, No. 1, Article 2, 2012.

[18] Somvanshi, P., Rane, M.. "Survey of Palmprint Recognition". International Journal of Scientific & Engineering Research, 3 (2), 2012

[19] Kong, A., Zhang, D., Kamel M., "A survey of palmprint recognition". Pattern Recognition 42 pp:1408-1418, 2009.

[20] Lu, G., Zhang, D., A and Wang, K. 2003. Palmprint recognition using eigenpalms features. *Pattern Recog. Lett. 24,* 9, 1463–1467.

[21] Ribaric, S. and Fratric, I. 2005. A biometric identification system based on eigenpalm and eigenfinger features. *IEEE Trans. Pattern Anal. Mach. Intell. 27,* 11, 1698–1709.

[22] Connie, T., Jin, A., Ong, M., and Ling, D. 2003. An automated palmprint recognition system. *Image Vis. Comput. 23,* 5, 501–515.

[23] Yang, J., Zhang, D., Yang, J., and Niu, B. 2007. Globally maximizing, locally minimizing: Unsupervised discriminant projection with applications to face and palm biometrics. *IEEE Trans. Pattern Anal. Mach. Intell. 29,* 4, 650–664.

[24] Wu, X., Zhang, D., And Wang, K. 2003. Fisherpalms based palmprint recognition. *Pattern Recog. Lett. 24*, 15, 2829–2838.

[25] Ekinci, M. and Aykut , M. 2007. Gabor-based kernel pca for palmprint recognition. *Electron. Lett. 43,* 20, 1077–1079.

[26] Wang, Y. and Ruan, Q. 2006b. Kernel fisher discriminant analysis for palmprint recognition. In *Proceed- ings of the 18th International Conference on Pattern Recognition*. 457–460.

[27] Zou, W., Zhang, D., and Wang, K. 2006b. Bi-directional pca with assembled matrix distance metric for image recognition. *IEEE Trans. Syst. Man Cybern.* Part B: Cybernetics *36,* 4, 863–872.

[28] Hu, D., Feng, G., and Zhou, Z. 2007. Two-dimensional locality preserving projection (2dlpp) with its application to palmprint recognition. *Pattern Recog. 40,* 1, 339–342.

[29] Jing, X. and Zhang, D. 2004. A face and palmprint recognition approach based on discriminant dct feature extraction. *IEEE Trans. Syst. Man Cybern.* Part B: Cybernetics *34,* 6, 2405–2415.

[30] Jing, X., Tang, Y., and Zhang, D. 2005. A fourier-lda approach for image recognition. *Pattern Recog. 38,* 3, 453–457.

[31] Li, W., You, J., and Zhang, D. 2005. Texture-based palmprint retrieval using a layered search scheme for personal identification. *IEEE Trans. Multimedia 7,* 5, 891–898.

[32] Noh, J. and Rhee, K. 2005. Palmprint identification algorithm using hu invariant moments and otsu binarization. In *Proceedings of the 4th International Conference on Computer and Information Science*. 94–99.

[33] Zhang, L. and Zhang, D. 2004. Characterization of palmprints by wavelet signatures via directional context modeling. *IEEE Trans. Syst. Man Cybern.* Part B *34*, 3, 1335–1347.

[34] Hennings, P., Savvides M., Kumar, B., Kamel, M., AND Campilho, A. 2005. Verification of biometric palmprint patterns using optimal trade-off filter classifiers. In *Proceedings of the International Confer- ence on Image Analysis and Recognition*. 1081–1088.

[35] Hennings-Yeomans, P., Kumar, B. V., and Savvides, M. 2007. Palmprint classification using multi- ple advanced correlation filters and palm-specific segmentation. *IEEE Trans. Inf. Forensics Secur. 2*, 3, 613–622.

[36] WU, X., Zhang, D., and Wang, K. 2006b. Palm line extraction and matching for personal authentication. *IEEE Trans. Syst. Man Cybern.* Part A *36*, 5, 978–987.

[37] Liu, L., Zhang, D., and You, J. 2007. Detecting wide lines using isotropic nonlinear filtering. *IEEE Trans. Image Process. 16*, 6, 1584–1595.

[38] Gao, Y. and Leung, M. 2002. Face recognition using line edge map. *IEEE Trans. Pattern Anal. Mach. Intell. 24*, 6, 764–779.

[39] Zhang, D., Kong, W. K., You, J., and Wong, M. 2003. Online palmprint identification. *IEEE Trans.* Pattern Anal. Mach. Intell. 25, 9, 1041–1050.

[40] Kong, A., Zhang, D., and Kamel, M. 2006b. A study of brute-force break-ins of a palmprint verification system. *IEEE Trans. Syst. Man Cybern.* Part B *36*, 5, 1201–1205.

[41] Jia, W., Huang, D., and Zhang, D. 2008. Palmprint verification based on robust line orientation code. Pattern Recog. 41, 5, 1504–1513.

[42] KONG, A. AND Zhang, D. 2004. Competitive coding scheme for palmprint verification. In *Proceedings of the 17th International Conference on Pattern Recognition*. 520–523.

[43] Sun, Z., Tan, T., Wang, Y., and Li, S. 2005. Ordinal palmprint representation for personal identification. In *Proceedings of the International Conference on Computer Vision and Pattern Recognition*. 279–284.

[44] Wang, X., Gong, H., Zhang, H., LI, B., and Zhuang, Z. 2006. Palmprint identification using boosting local binary pattern. In *Proceedings of the International Conference on Pattern Recognition*. 503–506.

[45] Kumar, A. and Zhang, D. 2006. Personal recognition using hand shape and texture. *IEEE Trans. Image Process. 15*, 8, 2454–2461.

[46] Kumar, A. and Zhang, D. 2005. Personal authentication using multiple palmprint representation. *Pattern Recog. 38,* 10, 1695–1704.

[47] LI, Y., Wang, K., and Zhang, D. 2005. Palmprint recognition based on translation invariant zernike mo- ments and modular neural network. In *Lecture Notes on Computer Science* vol. 3497, 177–182.

[48] You, J., Kong, W., Zhang, D., and Chenung, K. 2004. On hierarchical palmprint coding with multiple features for personal identification in large databases. *IEEE Trans. Circuits Syst. Video Technol. 14,* 2, 234–243.

[49] Serratosa, F. Solé, A. 2008. "Biometría". Material Docente de la UOC. Spain.

[50] Paul S. Wu and Ming Li, "Pyramid edge detection based on stack filter", *Pattern Recognition Letters,* vol. 18, no. 4, pp. 239-248, 1997.

[51] Ratha N. K., Karu K., Chen S., Jain A.K. 1996. "A Real-Time Matching System for Large Fingerprint Databases," IEEE Transactions on Pattern Analysis and Machine Intelligence, 18 (8), pp. 799−813.

[52] Liu E, Jain A, and Tian J. 2013. A coarse to fine minutiae-based latent palmprint matching:http://biometrics.cse.msu.edu/Publications/Palmprints/LiuJainTian_Coarse2FineMinutiaeBasedLatentPalmprintMatching_PAMI13.pdf

[53] Jain, A. and Demirkus, M. 2008. On latent palmprint matching. technical report. http://biometrics.cse.msu.edu/Publications/Palmprints/ OnLatentPalmprintMatchingJainDemirkus08.pdf.

[54] Jain, A. K., Feng, J. 2009. "Latent Palmprint Matching". IEEE Transactions on Pattern Analysis and Matching Intelligence.

[55] Dai, J and Zhou, J. 2011. "Multifeature-Based High-Resolution palmprint recognition". IEEE Trnas. Pattern analysis and Machine Intelligence, Vol 33, No 5, pp. 945-957.

[56] Dai, J., Feng, J., Zhou, J. 2012. "Robust and Efficient Ridge Based Palmprint Matching", IEEE Transactions on Pattern Analysis and Matching Intelligence. 34 (8), pp. 1618-1632.

[57] Cappelli, R. Ferrara M. and Maio D, 2012. "A fast and accurate palmprint recognition system based on minutiae". Transactions on System, Man and Cyberbetics, Part B: Cybernetics, vol 42(3), pp. 956-962

[58] Anil K. Jain, Patrick Flynn, Arun A. Ross, "Handbook of Biometrics", Springer, 2009.

[59] Ballard, D.H.: "Generalizing the Hough Transform to Detect Arbitrary Shapes", Ridge Based Palmprint Matching", IEEE Trans. on Pattern Analysis and Matching Intelligence ., 1980.

[60] J. Funada, *et. al*., "Feature Extraction Method for Palmprint Considering Elimination of Creases," Proc. 14th Int. Conf. Pattern Recognition, pp. 1849-1854, 1998.